Quaternary International 398 (2016) 159–174

Contents lists available at ScienceDirect

Quaternary International

journal homepage: www.elsevier.com/locate/quaint

The Qesem Cave hominin material (part 1): A morphometric analysis of the mandibular premolars and molar

Gerhard W. Weber [a, b, *], Cinzia Fornai [a], Avi Gopher [c], Ran Barkai [c], Rachel Sarig [d, e], Israel Hershkovitz [d, f]

[a] University of Vienna, Department of Anthropology, Austria
[b] University of Vienna, Core Facility for Micro-Computed Tomography, Austria
[c] Tel Aviv University, Institute of Archaeology, Israel
[d] Dan David Center for Human Evolution and Biohistory, The Steinhardt Museum of Natural History and National Research Center, Tel Aviv University, Israel
[e] The Department of Orthodontics, The Maurice and Gabriela Goldschleger School of Dental Medicine, Tel Aviv University, Israel
[f] The Department of Anatomy and Anthropology, The Sackler Faculty of Medicine, Tel Aviv University, Israel

ARTICLE INFO

Article history:
Available online 9 February 2016

Keywords:
Dental morphometrics
Mid-Pleistocene
Late-Pleistocene
Neanderthals
Anatomically modern humans
Virtual Anthropology

ABSTRACT

The Mid-Pleistocene Qesem Cave near Tel Aviv in Israel yielded several hominin teeth and abundant faunal and cultural remains. The geological sequences of the cave were dated to 420,000–200,000 years ago. In this contribution, we focus on the three lower postcanine teeth which are among the oldest material from the cave. We used both Geometric Morphometrics and qualitative observations on the outer enamel surface and the internal enamel–dentine junction to investigate shape and size variation in a sample of Early-to Late-Pleistocene fossils (Sangiran, Mauer, Bilzingsleben, Ehringsdorf, Qafzeh, Ohalo), Neanderthals, and geographically diverse recent humans. Our approach based on three dental traits from three tooth types is able to distinguish quite well between dental specimens from anatomically modern humans (AMH) and Neanderthals (NEA). It also confirms an intermediate morphology of Mid-Pleistocene specimens in general, and the close proximity of Ehringsdorf to NEA. While the Qesem premolars display an intermediate shape between NEA and AMH, their size is definitely modern-like. The Qesem molar features a morphology and size closer to NEA. A possible explanation is the evolutionary dissociation of size and shape in premolars, and molars that are morphologically closer to NEA than premolars. It can be noted that a Mid-Pleistocene hominin population was present in Southwestern Asia that shows some Neanderthal affinities, probably more than Mauer and Bilzingsleben, but less than Ehringsdorf. With the current data, however, we cannot confidently assign the Qesem teeth to any existing taxon, nor exclude that it is an autochthonous phenomenon in the Levant.

1. Introduction

The Mid-Pleistocene is undoubtedly one of the most interesting epochs in human evolution, and at the same time one of the most enigmatic. It was characterized by alternating glacial and interglacial stages, accompanied by numerous short but severe climatic oscillations within these stages. While ice shields expanded, vegetation zones shifted southwards, and likely also human occupation in harsh regions disappeared, respectively, were limited to southern refugia (Dennell et al., 2011). In contrast, in warmer periods hominins survived as far north as Suffolk in East Anglia, 52° N (Parfitt et al., 2010). While we have not more than vague ideas how the genus *Homo* evolved in this phase of changing environmental conditions, we know that towards the late Mid-Pleistocene two different human demes appeared in the Old World: Neanderthals (NEA), and anatomically modern humans (AMH).

The hominin fossil record of the Mid-Pleistocene is characterized by a high morphological variability, sometimes referred to as the "muddle in the middle" (Harvati et al., 2010; Buck and Stringer, 2014). Fossil findings from this period are regarded by some as members of *Homo heidelbergensis*, but a clear definition of this taxon is lacking (Stringer, 2012). Specimens from Africa (e.g., Bodo, Kabwe, Elandsfontein, Ndutu), Asia (e.g., Dali, Jinniushan, Yunxian),

* Corresponding author. Department of Anthropology & Core Facility for Micro-Computed Tomography, University of Vienna, Althanstr. 14, A-1090 Wien, Austria.
E-mail address: gerhard.weber@univie.ac.at (G.W. Weber).
URL: http://www.anthropology.at/people/gweber

http://dx.doi.org/10.1016/j.quaint.2015.10.027
1040-6182/

and Europe (e.g., Mauer, Petralona, Arago, Bilzingsleben) show a mosaic of primitive and derived features to a different extent and are lumped into this taxonomical container by some, but not all authors (see Stringer, 2012 and references therein).

Whether Neanderthals developed via a gradual "accretion process" based mainly on genetic drift which requires partial or complete isolation (Hublin, 1998; Harvati et al., 2010), or via a model involving selection and continued genic exchange with other populations (Hawks and Wolpoff, 2001), is unclear. The approximate timeframe when NEA and AMH demes separated can be estimated using morphological or genetic data. Gómez-Robles et al. (2013), for instance, find no suitable candidate for the last common ancestor in the fossil record, but hypothesized that a European clade originated around 1 million years ago. Based on genetic data, the split between the populations leading to modern humans and Neanderthals is placed within the Mid-Pleistocene [370 thousand years ago (ka) (Noonan et al., 2006); 440–270 ka (Green et al., 2010); 480–425 ka (Endicott et al., 2010); 589-553 ka (Prüfer et al., 2014)] but the taxonomy of the last common ancestor to NEA and AMH remains undetermined. The *Homo* remains from Sima de los Huesos (SH; Spain), currently dated to 427 ka (Arnold et al., 2014), show very close morphological relationships with Neanderthals (Martinón-Torres et al., 2012). As Stringer (2012) stated, reclassifying the SH material as an early form of *H. neanderthalensis* would remove most of the data supporting a European chronospecies of *H. heidelbergensis-H.neanderthalensis*.

While it remains also unclear whether a potential last common ancestor of NEA and AMH might be found in Africa, Europe, or Asia (Rightmire, 2008; Martinon-Torres et al., 2011; Meyer et al., 2012; Stringer, 2012), or if a continuing admixture of several populations from different regions, probably under source-sink dynamics (Eller et al., 2004; Dennell et al., 2011), led to the two demes, the Levant – located at the crossroads between the three continents – is geographically a potential play ground for these developments. Doubts have nevertheless been raised (Martinón-Torres et al., 2011) if a passage from sub-Saharan Africa to the Levant might have been possible in the time frame between 500 and 300 ka due to the large desert areas in north-east Africa. Still, the unique geographical position of the Levant could have allowed admixture of longitudinally migrating population streams between Europe and Asia, and yet also Africa, if a passage was possible. To further complicate the picture, another recently defined hominin group has appeared in Asia, the Denisovans (Reich et al., 2010). They exist rather as a genetic construct than as a morphologically evident taxon, but they seem to be closer related to Neanderthals (and SH; Meyer et al., 2012) than to modern humans. Geneticists calculated a split time between Denisovans and Neanderthals roughly at 380 ka (Prüfer et al., 2014). Their origin is undetermined, but we cannot exclude that Denisovans, or their immediate precursors, inhabited the Levant. Southwestern Asia is also interesting from another, much later, perspective: It is the home of some of the first anatomically modern humans which were found outside Africa [Skhul, Qafzeh, ~120–90 ka (Mercier et al., 1993)], and at the same time it is the home of those Neanderthals [Tabun, 122 ka (Grün and Stringer, 2000, but could be younger); Kebara 60 ka (Schwarcz et al., 1989); Amud 70–50 ka (Valladas et al., 1999)] that were found geographically closest to Africa (which they never reached, according to our fossil record).

Recently, the Mid-Pleistocene Qesem Cave (QC) near Tel Aviv in Israel has yielded several hominin teeth and abundant faunal, as well as cultural remains. The stratigraphic sequence present at the cave was dated between 420 and 200 ka (Gopher et al., 2010; Mercier et al., 2013). The hominins at QC are associated with the Acheulo-Yabrudian Cultural Complex (Barkai et al., 2009; Barkai and Gopher, 2013). A first description of eight teeth has been published by Hershkovitz et al. (2011). Based on qualitative assessments and traditional linear measurements they already pointed out the ambiguous morphological affinities of the Qesem teeth to anatomically modern humans and Neanderthals. Since then, additional five isolated teeth were found in the cave (Hershkovitz et al., 2016). One of them is a right lower second molar which is described and used in this contribution.

We focus on the mandibular third and fourth premolar (P_3 and P_4, respectively) from one individual (Hershkovitz et al., 2011), dated to about 350 ka, and a lower second molar (M_2) from another individual, which at least post-dates 300 ka (Fig. 2). The reason is that these three teeth represent some of the oldest material from the Qesem cave. We use 3D geometric morphometric methods which capture the external and internal geometry of the teeth. This allows analyses of shape and size independent from each other. Our goal is a thorough quantitative description of the 3D geometry of the three QC teeth, and a morphological comparative study with other Pleistocene and Holocene material. Our approach is a phenetic rather than a cladistics one. Given the diffuse picture of Mid-Pleistocene human evolution in general, we do not aim at a definite taxonomic classification at this point.

2. Materials and methods

The sample (Table 1) consists of the three teeth from Qesem Cave P_3-QC9, P_4-QC10, and M_2-QC12, several Neanderthals from Europe and the Levant, Late-Pleistocene (~127–10 ka[1]) anatomically modern humans from the Levant, epipaleolithic Natufians, and a quite diverse sample of recent modern human populations from various geographic regions, among them Khoesan, Papuans, Australian aboriginals, Middle Europeans, Avars (7^{th}–8^{th} century Euro-Asian nomads), and recent Bedouins from Israel. The accessibility of high-resolution 3D data of well-preserved teeth from the Mid-Pleistocene (~781–127ka[1]) is unfortunately very low. Teeth are either missing, or broken, too worn, of a different tooth type, or simply not accessible to us or for scanning in general. Nevertheless, we could consider some Early- (>781 ka[1]) to Mid-Pleistocene lower premolars and molars, including Mauer (the type specimen of *Homo heidelbergensis*), Bilzingsleben E6[2] (*Homo heidelbergensis* or *Homo erectus*; see Vlcek et al., 2002; Stringer, 2012), Ehringsdorf F and G [early Neanderthals according to their old age (Grün et al., 1988; van Asperen, 2012) and their near-Neanderthal or transitional morphology, see e.g. Vlcek (1993) and Smith (1984)], and some Sangiran (S7) Javanese *Homo erectus*.

The QC teeth and most of the comparable material were μCT-scanned at the Core Facility for Micro-Computed Tomography at University of Vienna with a custom built VISCOM X8060 (Germany) μCT scanner with slightly differing scan parameters (adjusted for each specimen): 140–160 kV, 300–400 μA, 1400–2000msec, diamond high performance transmission target, 0.75 mm copper filter, isometric voxel sizes between 9 and 44 μm. X-ray images were taken from 1440 different angles. Using filtered back-projection in VISCOM XVR-CT 1.07 software, these data were reconstructed as 3D volumes with a colour depth of 16,384 grey values. The Ehringsdorf and Bilzingsleben specimens were made available for scanning by the Thüringisches Landesamt für Denkmalpflege und Archäologie Weimar, all the Israeli material by the Tel Aviv University. Other comparable data were obtained from existing collections and data

[1] http://quaternary.stratigraphy.org/definitions/pleistocenesubdivision/.

[2] The Bilzingsleben E6 specimen is still partly embedded in a stone matrix and not extensively described. It was only classified as "lower P1-2 sin." by Vlcek (2011). Looking at its morphology after virtual removal from the stone matrix, we assess the specimen as a left lower P_4.

Table 1
Sample composition Qesem Cave.

Tab.1: Sample composition Qesem Cave

Lower P3						Lower P4						Lower M2					
Abbrev.	Specimen	Taxon	Cerv	Crown	EDJ	Abbrev.	Specimen	Taxon	Cerv	Crown	EDJ	Abbrev.	Specimen	Taxon	Cerv	Crown	EDJ
Early and Middle Pleistocene																	
QC_G22	P3-QC9	Indetermined	x	x	x	QC_G22	P4-QC10	Indetermined	x	x	x	QC_J15	M2-QC12	Indetermined	x	x	x
Mauer	Mauer Heidelberg	*H. heidelbergensis*	x	x	x	Mauer	Mauer Heidelberg	*H. heidelbergensis*	x	x	x	Mauer	Mauer Heidelberg	*H. heidelbergensis*	x	x	x
SMF-S7-25	Sangiran S7-25	*H. erectus*	x	x		Bilzingslb	Bilzingsleben E6	*?H. heidelbergensis*	x	x	x						
SMF-S7-26	Sangiran S7-26	*H. erectus*	x	x													
SMF-S7-69	Sangiran S7-69	*H. erectus*	x	x													
Ehrings_F	Ehringsdorf F	*Early-Neanderthal*	x	x		Ehrings_F	Ehringsdorf F	*Early-Neanderthal*	x			Ehrings_F	Ehringsdorf F	*Early-Neanderthal*	x		
Ehrings_G	Ehringsdorf G	*Early-Neanderthal*	x	x	x	Ehrings_G	Ehringsdorf G	*Early-Neanderthal*	x	x	x	Ehrings_G	Ehringsdorf G	*Early-Neanderthal*	x	x	x
Late Pleistocene and Holocene																	
Amud1	Amud 1	*H. neanderthalensis*	x	x		Amud1	Amud 1	*H. neanderthalensis*	x	x		Amud1	Amud 1	*H. neanderthalensis*	x	x	
LaQuina5	La Quina H5	*H. neanderthalensis*	x	x		LaQuina5	La Quina H5	*H. neanderthalensis*	x	x	x	Kebara2	Kebara 2	*H. neanderthalensis*	x	x	
NEA_Kr-d25	Krapina 25	*H. neanderthalensis*	x	x	x	NEA_Kr-d26	Krapina 26	*H. neanderthalensis*	x	x	x	LaQuina5	La Quina H5	*H. neanderthalensis*	x	x	
NEA_Kr-d27	Krapina 27	*H. neanderthalensis*	x	x		NEA_Kr-d30	Krapina 30	*H. neanderthalensis*	x	x	x	Tabun2	Tabun 2	*H. neanderthalensis*	x		
NEA_Kr-d28	Krapina 28	*H. neanderthalensis*	x	x		NEA_Kr-d31	Krapina 31	*H. neanderthalensis*	x	x	x	NEA_Kr-d2	Krapina 2	*H. neanderthalensis*	x	x	
NEA_Kr-d29	Krapina 29	*H. neanderthalensis*	x	x	x	NEA_Kr-d33	Krapina 33	*H. neanderthalensis*	x	x	x	NEA_Kr-d3	Krapina 3	*H. neanderthalensis*	x		x
NEA_Kr-d32	Krapina 32	*H. neanderthalensis*	x	x	x	NEA_Kr-d35	Krapina 35	*H. neanderthalensis*	x	x	x	NEA_Kr-d6	Krapina 6	*H. neanderthalensis*	x	x	x
NEA_Kr-d34	Krapina 34	*H. neanderthalensis*	x	x	x	NEA_Kr-d113	Krapina 113	*H. neanderthalensis*	x	x	x	NEA_Kr-d10	Krapina 10	*H. neanderthalensis*	x	x	x
Qafzeh9	Qafzeh 9	Anat. Modern *Homo*	x	x	x	Qafzeh9	Qafzeh 9	Anat. Modern *Homo*	x	x	x	NEA_Kr-d86	Krapina 86	*H. neanderthalensis*	x	x	x
Qafzeh11	Qafzeh 11	Anat. Modern *Homo*	x	x	x	Qafzeh11	Qafzeh 11	Anat. Modern *Homo*	x	x	x	NEA_Kr-d104	Krapina 104	*H. neanderthalensis*	x	x	x
NAT_AM57	Ain Mallaha 57	*Natufian, Israel*	x	x	x	NAT_AM55	Ain Mallaha 55	*Natufian, Israel*	x	x	x	NEA_Kr-d107	Krapina 107	*H. neanderthalensis*	x	x	x
NAT_AM87	Ain Mallaha 87	*Natufian, Israel*	x	x	x	NAT_AM57	Ain Mallaha 57	*Natufian, Israel*	x	x	x	Ohalo1	Ohalo 1	Anat. Modern *Homo*	x		
NAT_AM88	Ain Mallaha 88	*Natufian, Israel*			x	NAT_AM91	Ain Mallaha 91	*Natufian, Israel*	x		x	Ohalo2	Ohalo 2	Anat. Modern *Homo*	x	x	
NAT_AM91	Ain Mallaha 91	*Natufian, Israel*	x	x	x	NAT_Hay02	Hayonim 02	*Natufian, Israel*	x	x	x	Qafzeh9	Qafzeh 9	Anat. Modern *Homo*	x	x	x
NAT_Hay02	Hayonim 02	*Natufian, Israel*	x	x		NAT_Hay09	Hayonim 09	*Natufian, Israel*	x	x	x	Qafzeh11	Qafzeh 11	Anat. Modern *Homo*	x	x	x
NAT_Hay09	Hayonim 09	*Natufian, Israel*	x	x	x	NAT_Hay12	Hayonim 12	*Natufian, Israel*	x	x	x	Qafzeh15	Qafzeh 15	Anat. Modern *Homo*	x	x	x
NAT_Hay12	Hayonim 12	*Natufian, Israel*	x	x	x	NAT_Hay13	Hayonim 13	*Natufian, Israel*	x	x	x	NAT_AM55	Ain Mallaha 55	*Natufian, Israel*	x	x	x
NAT_Hay13	Hayonim 13	*Natufian, Israel*	x	x	x	NAT_Hay28	Hayonim 28	*Natufian, Israel*	x	x	x	NAT_AM57	Ain Mallaha 57	*Natufian, Israel*	x	x	x
NAT_Hay28	Hayonim 28	*Natufian, Israel*	x	x	x	RHS_C109	Modern Homo	Recent, Australia	x	x	x	NAT_AM87	Ain Mallaha 87	*Natufian, Israel*	x	x	x
RHS_C109	Modern Homo	Recent, Australia	x	x	x	RHS_CN5	Modern Homo	Recent, Papua-NG	x	x	x	NAT_AM88	Ain Mallaha 88	*Natufian, Israel*			x
RHS_CN5	Modern Homo	Recent, Papua-NG	x	x		RHS_CN230	Modern Homo	Recent, Papua-NG	x	x	x	NAT_AM91	Ain Mallaha 91	*Natufian, Israel*	x	x	
RHS_CN230	Modern Homo	Recent, Papua-NG	x	x	x	RHS_CN232	Modern Homo	Recent, Papua-NG	x	x	x	NAT_Hay02	Hayonim 02	*Natufian, Israel*	x	x	
RHS_CN232	Modern Homo	Recent, Papua-NG	x	x		RHS_CN236	Modern Homo	Recent, Papua-NG	x	x	x	NAT_Hay09	Hayonim 09	*Natufian, Israel*			x
RHS_CN236	Modern Homo	Recent, Papua-NG	x	x	x	RHS_Cs428	Modern Homo	Historic, Europe	x	x	x	NAT_Hay12	Hayonim 12	*Natufian, Israel*	x	x	x
RHS_Cs428	Modern Homo	Historic, Europe	x	x		RHS_Cs495	Modern Homo	Historic, Europe	x	x	x	NAT_Hay13	Hayonim 13	*Natufian, Israel*	x	x	x
RHS_Cs495	Modern Homo	Historic, Europe	x	x	x	RHS_Cs498	Modern Homo	Historic, Europe	x	x	x	NAT_Hay28	Hayonim 28	*Natufian, Israel*	x	x	x
RHS_Cs498	Modern Homo	Historic, Europe	x	x		RHS_Cs502	Modern Homo	Historic, Europe	x	x	x	RHS_C109	Modern Homo	Recent, Australia	x	x	x
RHS_Cs502	Modern Homo	Historic, Europe	x	x	x	RHS_Cs541	Modern Homo	Historic, Europe	x	x	x	RHS_CN232	Modern Homo	Recent, Papua-NG	x	x	x
RHS_Cs541	Modern Homo	Historic, Europe	x	x	x	RHS_S4	Modern Homo	Recent, Africa	x	x	x	RHS_140	Modern Homo	Recent, Europe	x	x	x
RHS_ID120	Modern Homo	Recent, Europe	x	x	x	RHS_S5	Modern Homo	Recent, Africa	x	x	x	RHS_S4	Modern Homo	Recent, Africa	x	x	x
RHS_ID300	Modern Homo	Recent, Europe	x	x	x	RHS_S23	Modern Homo	Recent, Africa	x	x	x	RHS_S16	Modern Homo	Recent, Africa	x	x	x
RHS_S4	Modern Homo	Recent, Africa	x	x	x	RHS_S81	Modern Homo	Recent, Africa	x	x	x	RHS_S46	Modern Homo	Recent, Africa	x	x	x
RHS_S5	Modern Homo	Recent, Africa	x	x	x	RHS_S89	Modern Homo	Recent, Africa	x	x	x	RHS_S86	Modern Homo	Recent, Africa	x	x	x
RHS_S23	Modern Homo	Recent, Africa	x	x	x	RHS_S103	Modern Homo	Recent, Africa	x	x	x	RHS_S126	Modern Homo	Recent, Africa	x	x	
RHS_S81	Modern Homo	Recent, Africa	x	x	x	RHS_S121	Modern Homo	Recent, Africa	x	x	x	BLZ_004	Modern Homo	Recent, Bedouin	x	x	x
RHS_S89	Modern Homo	Recent, Africa	x	x	x	RHS_S126	Modern Homo	Recent, Africa	x	x	x	BLZ_014	Modern Homo	Recent, Bedouin	x	x	x
RHS_S103	Modern Homo	Recent, Africa	x	x	x	BLZ_004	Modern Homo	Recent, Bedouin	x	x	x	BLZ_026	Modern Homo	Recent, Bedouin	x	x	x
RHS_S121	Modern Homo	Recent, Africa	x	x	x	BLZ_014	Modern Homo	Recent, Bedouin	x	x	x	BLZ_037	Modern Homo	Recent, Bedouin	x	x	x
RHS_S126	Modern Homo	Recent, Africa	x	x	x	BLZ_026	Modern Homo	Recent, Bedouin	x	x	x	EAR_H298	Modern Homo	Recent, Bedouin	x	x	x
BLZ_004	Modern Homo	Recent, Bedouin	x	x	x	BLZ_037	Modern Homo	Recent, Bedouin	x	x	x						
BLZ_014	Modern Homo	Recent, Bedouin	x	x	x	EAR_H298	Modern Homo	Recent, Bedouin	x	x	x						
BLZ_026	Modern Homo	Recent, Bedouin	x	x	x												
BLZ_037	Modern Homo	Recent, Bedouin	x	x	x												
EAR_H298	Modern Homo	Recent, Bedouin	x	x	x												

bases (Ruprecht Karls Universität Heidelberg, NESPOS Data Base, Senckenberg Research Institute Frankfurt, the Croatian Natural History Museum Zagreb, the Muséum National d'Histoire Naturelle Paris, AST-RX - Plateau technique d'imagerie tomographique RX the Max-Planck Institute Leipzig). All teeth were standardized to left ones, i.e. right ones were mirrored. If both antimeres were present in a specimen, the better preserved one was chosen. The post-processing of the image stack was performed in AMIRA 5.6 (Mercury Computer Systems, Chelmsford, USA), and surface models of the outer enamel surface (OES) and enamel–dentine junction (EDJ) were produced after segmentation of the volume data. All data operations follow in principle the guidelines described in the textbook "Virtual Anthropology" (Weber and Bookstein, 2011, see also summary in Weber (2015)).

For teeth worn up to grade 3 of Molnar's classification (1971), a minimal reconstruction of the horn tips was performed (if only 0.2 mm – 0.8 mm in height were missing). Specimens with heavier wear were not considered for this investigation. Unfortunately the quality of scans of the Sangiran material did not allow any separation of the enamel from the dentine. They were thus excluded from the EDJ analysis (see Table 1). Landmark data were collected from 3D virtual models of the dental crowns. We used Geometric Morphometric methods based on landmarks and semilandmarks in 3D (not from photographs) to examine shape and form (Weber and Bookstein, 2011; Weber, 2015) of three different dental traits:

1) the enamel-dentine-junction (EDJ),
2) the cervical outline, and
3) the crown outline.

The use of cervical and crown outlines permits the inclusion of those teeth that showed strongly affected occlusal surfaces by dental wear or damage.

For the EDJ, the following protocol was used (Fig. 1): Four landmarks were identified on P_3s and P_4s: protoconid horn tip, metaconid horn tip, deepest point of the mesial fossa, deepest point

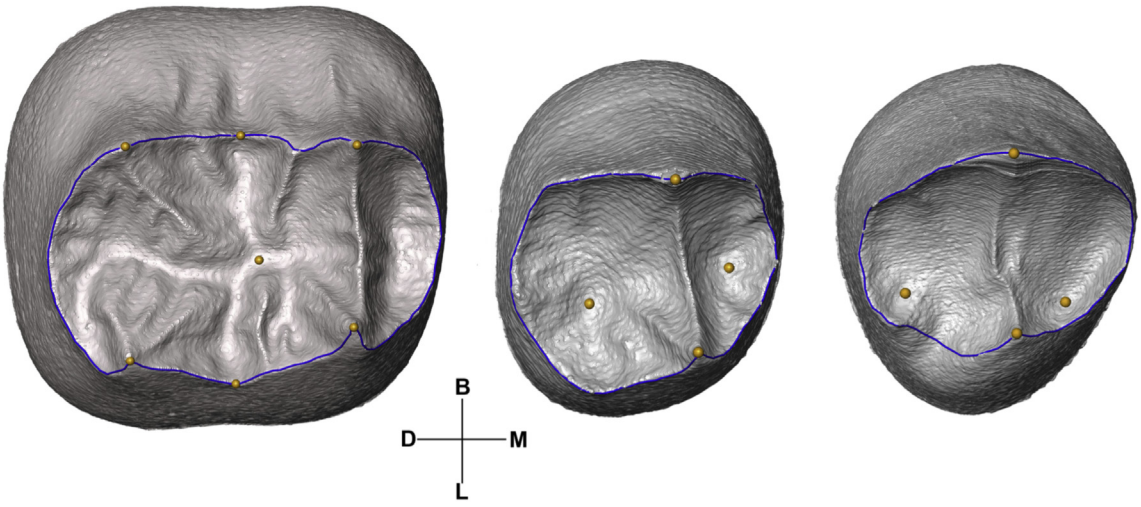

Fig. 1. Landmarks (yellow spheres) and curves (blue) on the EDJ of lower M_2s (left), P_4s (middle), and P_3s (right). All specimens represent the actual Qesem specimens, the right molar was mirrored to be a left one. B – buccal; M– mesial; L – lingual; D – distal. (For interpretation of the references to colour in this figure legend, the reader is referred to the web version of this article.)

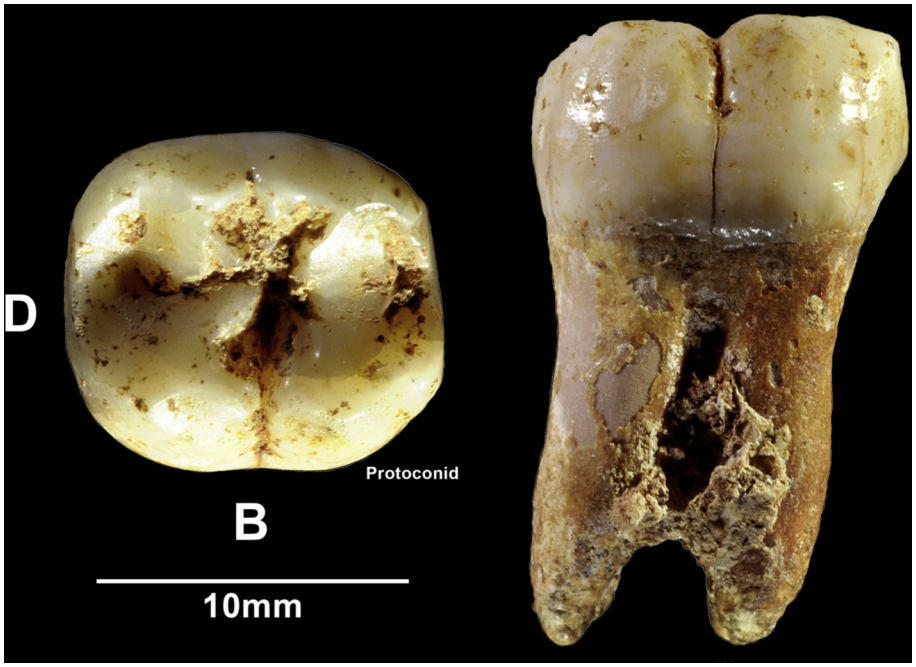

Fig. 2. Qesem right lower second molar M_2-QC12 in occlusal (left) and buccal (right) view.

of the distal fossa. Eight semilandmarks were identified on the mesial marginal ridge, 13 semilandmarks on the distal marginal ridge. For M_2s, seven landmarks were used: The horn tips of the protoconid, metaconid, hyponid, entoconid, the deepest point of the central fossa, and of the buccal and lingual fissure. In addition, 22 semilandmarks were identified along the whole occlusal ridge of the EDJ. Landmarks and curves were created in the Templand partition of the EVAN Toolbox 1.71 (ET; http://evan-society.org), where the sliding of the semilandmarks is based on the minimum bending energy approach (Bookstein, 1989; Gunz et al., 2005; Gunz and Mitteroecker, 2013).

For cervical and crown outline analyses, we followed the instruction published in Benazzi et al., 2012, with some modifications (Fig. S1). The surface data of the dental crown (OES and EDJ) were imported into RapidForm XOR2 (INUS Technology) and realigned so that the best fit plane at the cervical margins was parallel to the XY plane. Premolars were subsequently rotated in such a way that the buccal ridge of the EDJ was aligned parallel with the X-axis, molars were rotated to align the lingual margin parallel to the X-axis (Fig. S1 a&b). The crown and cervical outlines of each tooth were collected and projected onto the respective cervical plane. The crown outline thus corresponds to the silhouette of the oriented tooth, as seen in occlusal view. The cervical outline represents the perimeter of the dental crown at the intersection with the cervical plane. The outlines were then transferred to Rhinoceros 4.0 Beta CAD environment (Robert McNeel & Associates, Seattle, WA). The centroid for each outline area was calculated and 24 equiangularly (15°) spaced radii were

drawn counter-clockwise. The intersection of the 24 radii with each outline resulted in 24 pseudolandmarks (in contrast to 16 in Benazzi et al., 2012).

The landmark configurations from cervical and crown outlines, and the EDJ surface, were treated separately in the GM analyses. A combination of EDJ with cervical outline, thus combining data from the base of the crown with data from the occlusal surface, would have further reduced the applicable data set because some interesting specimens, such as Sangiran, feature only outline data. Conversion of the Cartesian coordinates into shape variables eliminates variation in orientation, location, and size. This was done by means of a Generalized Procrustes Analysis (GPA; Gower, 1975; Marcus et al., 1996), which also separates shape from size. Shape variables (or form variables, if size is brought back; Mitteroecker et al., 2004) were then subjected to Principal Component Analysis (PCA) for reducing dimensions, and then shape/form changes were visualized by Thin Plate Spline warping (TPS; Bookstein, 1978, 1991). These tasks were performed in the EVAN Toolbox 1.71. For MANOVA permutation tests the software PAST (Hammer et al., 2001) was used, other statistics were performed in IBM SPSS Statistics 22 (IBM Corporation). Two-block Partial Least Squares analysis (PLS) was performed in the EVAN Toolbox 1.71. It is based on a singular value decomposition of the matrix of covariances between the two sets of variables. The results are pairs of linear combinations that successively maximize the covariance between the sets of variables, while being mutually uncorrelated across sets. Linear Discriminant Analysis (LDA) using the first ten principal components of PCA (accounting for roughly 90% of shape variance, or more) was performed in IBM SPSS Statistics 22 (IBM Corporation) to assess the predicted group membership of those specimens that were not clearly assigned to either “AMH” or “NEA”, and to determine the percentage of correctly classified cases for the defined groups. The leave-one-out approach was applied to those specimens in Table 2 that we considered clearly attributable to one of these two groups (Amud 1, Qafzeh 9, Qafzeh 11, Ohalo 1).

3. Results

A qualitative description of the two lower premolars (P_3-QC9, P_4-QC10) can be found in Hershkovitz et al. (2011). M_2-QC12 is described below (but see also Hershkovitz et al., 2016).

3.1. The right lower second molar M_2-QC12

M_2-QC12 (also referred to as QC_J15_540-550) was found in 2011 in square J/15, 540–550 cm below datum. It originates from an Amudian blade-dominated context and dates to c. 300 ka or somewhat later. The tooth is complete (Fig. 2), the apices of the roots are fused. The grooves and pits of the occlusal surface are partly covered by sedimentary concretion, as are parts of the roots, especially at the root bifurcation. These concretions were removed virtually (Weber and Bookstein, 2011) prior to the morphological description. There are several fine cracks visible on the mesial, lingual, and distal side walls of the crown, and only one severe crack on the buccal side, running from the buccal fissure to the cervical margin. The crown shows a rectangular outline (Fig. 2), its distal portion is not pointed. The occlusal surface is only minimally affected by wear, no dentine is exposed (maximum stage 2; Molnar, 1971). The distal slope of the entoconid, however, exhibits a deep enamel pit. The crown presents four cusps, and a hypoconulid is not present (Fig. 2; see also the dentine surface in Fig. 6 left). The sequence of cusp size is protoconid > hypoconid > metaconid > entoconid. No protostylid is visible. The mesial fossa is deep and anteriorly bounded by a continuous mesial marginal ridge. The longitudinal fissure is interrupted mesially (shortly after leaving the central fossa) by a strong middle trigonid crest on the enamel (ASUDAS 1B, Turner et al., 1991). The distal fossa is shallow and large, delimited by a sharp distal marginal ridge. Both interproximal contact facets (IPCF) are well developed, the mesial IPCF being fairly large in transverse direction and clearly inclined upwards (~116° in relation to the anterior occlusal surface). The mesial roots are fused, and so are the distal ones. There are two root canals mesially, but only a fused one distally. All roots are slightly curved distally and approximately of equal length. The bifurcation is rather high (43% of root length from cementoenamel junction, only visible on the electronically cleaned specimen, see also Fig. S2), the pulp chamber is unremarkably small, there is no sign of taurodontism. The taurodontism index (after Keene, 1966) results in TI = 18.56% which means cynodont (Fig. S2). Mesio-distal (M/D) diameter of the crown is 12.3 mm (uncorrected for IPCF), the bucco-lingual (B/L) diameter is 11.3 mm, crown height at the protoconid 7.4 mm, root length on the buccal aspect ~ 14.0 mm.

Although there is no absolute argument ruling out the possibility of a lower M_1 (a lower M_3 can be ruled out with high confidence based on the presence of mesial and distal IPCFs), we consider QC12 being a lower M_2 based on the following morphological evidence: there are only four cusps present; the tooth has a rectangular outline with no triangular distal extension; the tooth was markedly inclined forward when in place, as denoted by the angulation of the mesial IPCF, and the wear is mainly located mesially and distally rather than on the central basin, both as it would be expected for an M_2 in a normal functional dental relationship.

3.2. Geometric morphometric analyses

Owing to the preservational status of the individual specimens, not all of them could be included in all analyses. Table 1 provides an overview of the maximum sample for each tooth type. Form, shape, and size for three traits and three tooth types were analyzed separately. Accounting for the space limitations of this article, we cannot show all results in detail. We therefore focus on the most significant findings and summarize them (more details are provided in supplementary material).

3.2.1. Size

We observe a clear distinction of AMH and NEA in terms of size for all traits and tooth types. Highly significant differences in size (represented as lnCS in permutation tests, 10.000 samples) of P_3s for cervical outlines ($p < 0.001$), crown outlines ($p < 0.001$), and EDJ ($p < 0.001$) between AMH and NEA were found, where NEAs are always larger than AMHs. In the same way, AMH and NEA P_4s (cervical outlines $p < 0.001$; crown outlines $p = 0.002$; EDJ $p < 0.001$), and M_2s (cervical outlines $p < 0.001$; crown outlines $p < 0.001$; EDJ $p < 0.001$) showed highly significant size differences. Sizes for the three traits within a tooth type are significantly correlated (P_3 between 0.84 and 0.92, highest between cervical and crown outline; P_4 between 0.86 and 0.90, highest between crown outline and EDJ; M_2 between 0.81 and 0.90, highest between cervical and crown outline).

lnCS is hence a very distinctive parameter characterizing the lower premolars and the second molar of AMH on the one hand, and NEA on the other hand. The Qesem premolars are rather small in comparison to NEA (Fig. 3). They are almost always within the middle 50% (interquartile range - IQR) of AMH (with the only exception of P_3 EDJ). Qesem premolars are also always smaller than the Early-to Mid-Pleistocene material from Sangiran, Mauer, and Ehringsdorf. Only the P_4 EDJ of Bilzingsleben is smaller. Sangiran, Ehringsdorf, and Bilzingsleben (for the latter only cervical outline) are generally intermediate in size between AMH and NEA. In

Table 2
Results for the three traits of all three tooth types for QC and some selected Early, Mid, and Late Pleistocene specimens. The first five nearest neighbors (based on full Procrustes distances in shape space) of specimens (blue – AMH, pink – NEA, green – Early to Mid Pleistocene hominins) and the results of the linear discriminant analysis (LDA; % of correct classifications for AMH and NEA, classification for the respective specimen, probability for classification Ppost) are given.

P3 Cervical OL	QC	Mauer	Sangiran S7-25	Qafzeh 9	Qafzeh 11	Amud 1	Ehringsdorf G
	RHS_S121	NEA_Kr-d27	RHS_S23	NAT_AM_H57	RHS_Cs498	NAT_AM_H57	NEA_Kr-d28
	RHS_Cs541	Ehrings_F	SMF-S7-26	BLZ_014	BLZ_014	BLZ_004	NEA_Kr-d27
	EAR_H298	RHS_S121	RHS_S4	NAT_AM_H91	RHS_CN230	RHS_S89	Ehrings_F
	NAT_Hay_H02	NEA_Kr-d32	RHS_S5	RHS_S81	RHS_S103	RHS_S81	SMF-S7-25
	NEA_Kr-d29	RHS_S4_LP3	RHS_S126	Amud1	RHS_ID_300	EAR_H298	RHS_S121
Classif. LDA (100.0%, 87,5%)	AMH (Ppost=0.999)	NEA (Ppost=0.723)	AMH (Ppost=0.996)	AMH (Ppost=1.000)	AMH (Ppost=1.000)	AMH (Ppost=0.611)	NEA (Ppost=0.768)
P3 Crown OL	QC	Mauer	Sangiran S7-25	Qafzeh 9	Qafzeh 11	Amud 1	Ehringsdorf G
	RHS_S89	RHS_Cs498	SMF-S7-26	NAT_AM_H87	NAT_Hay_H02	Qafzeh_11	RHS_CN232
	NAT_AM_H87	NEA_Kr-d27	RHS_Cs541	NAT_Hay_H02	RHS_S5	NAT_AM_H91	RHS_S4
	Qafzeh9	NAT_HayH13	NAT_Hay_H09	RHS_S89	RHS_Cs502	NAT_Hay_H02	BLZ_026
	Amud1	NEA_Kr-d25	RHS_S23	NAT_AM_H57	Amud1	NAT_AM_H87	NEA_Kr-d29
	NAT_Hay_H02	BLZ_004	BLZ_037	RHS_ID_120	RHS_S103	RHS_CN230	NEA_Kr-d28
Classif. LDA (97.1%, 100.0%)	NEA (Ppost=0.519)	NEA (Ppost=0.943)	AMH (Ppost=1.000)	AMH (Ppost=1.000)	AMH (Ppost=0.739)	NEA (Ppost=0.930)	NEA (Ppost=0.535)
P3 EDJ	QC	Mauer	Sangiran S7-25	Qafzeh 9	Qafzeh 11	Amud 1	Ehringsdorf G
	RHS_S126	RHS_S81	-	RHS_CN230	BLZ_037	-	NEA_Kr-d29
	NEA_Kr-d29	BLZ_037	-	RHS_S5	RHS_S4	-	NEA_Kr-d25
	RHS_Cs502	NEA_Kr-d29	-	RHS_ID300	RHS_Cs502	-	NEA_Kr-d34
	NEA_Kr-d32	Qafzeh_11	-	NAT_AM_H57	RHS_S81	-	BLZ_026
	Ehrings_G	BLZ_026	-	NAT_AM_H91	BLZ_004	-	NEA_Kr-d32
Classif. LDA (96.8%, 100.0%)	AMH (Ppost=0.559)	AMH (Ppost=0.983)	-	AMH (Ppost=1.000)	AMH (Ppost=1.000)	-	NEA (Ppost=1.000)
P4 Cervical OL	QC	Mauer	Bilzingsleben E6	Qafzeh 9	Qafzeh 11	Amud 1	Ehringsdorf G
	Mauer	Bilzingsleben	Mauer	BLZ_014	NAT_AM_H57	RHS_S4	Ehrings_F
	Bilzingsleben	NEA_Kr-d26	QC_G22	BLZ_037	BLZ_014	NAT_Hay_H13	NEA_Kr-d113
	NEA_Kr-d30	NEA_Kr-d33	NEA_Kr-d33	RHS_CN232	NAT_AM_H55	NAT_Hay_H02	RHS_S89
	NEA_Kr-d33	QC_G22	NEA_Kr-d26	RHS_Cs428	LaQuina5	LaQuina5	NAT_Hay_H13
	NEA_Kr-d113	NEA_Kr-d113	NEA_Kr-d113	NAT_AM_H91	RHS_S23	NAT_Hay_H28	NEA_Kr-d33
Classif. LDA (93.8%, 100.0%)	NEA (Ppost=0.997)	NEA (Ppost=0.986)	NEA (Ppost=0.993)	AMH (Ppost=1.000)	AMH (Ppost=1.000)	NEA (Ppost=0.921)	NEA (Ppost=0.996)
P4 Crown OL	QC	Mauer	Bilzingsleben E6	Qafzeh 9	Qafzeh 11	Amud 1	Ehringsdorf G
	NAT_Hay_H28	NAT_HayH13	NEA_Kr-d33	RHS_S23	LaQuina5	Ehrings_G	Amud1
	BLZ_026	RHS_S103	EAR_H298	RHS_Cs495	NAT_AM_H57	NAT_Hay_H12	NEA_Kr-d113
	RHS_C109	NEA_Kr-d33	Mauer	BLZ_037	BLZ_004	Qafzeh_11	LaQuina5
	RHS_Cs541	RHS_S4	NAT_Hay_H13	RHS_Cs541	RHS_Cs498	RHS_Cs498	RHS_Cs498
	NAT_AM_H55	NAT_HayH28	RHS_S4	BLZ_004	NAT_Hay_H12	LaQuina5	Qafzeh_11
Classif. LDA (93.8%, 100.0%)	NEA (Ppost=0.914)	AMH (Ppost=0.598)	AMH (Ppost=0.991)	AMH (Ppost=0.976)	AMH (Ppost=0.981)	NEA (Ppost=0.894)	NEA (Ppost=1.000)

Table 2 *(continued).*

P4 EDJ	QC	Mauer	Bilzingsleben E6	Qafzeh 9	Qafzeh 11	Amud 1	Ehringsdorf G
	RHS_Cs502	NAT_HayH12	NAT_AM_H57	RHS_CN5	Ehrings_G	-	NEA_Kr-d33
	RHS_S81	RHS_S81	RHS_S5	BLZ_004	BLZ_014	-	NEA_Kr-d113
	NEA_Kr-d33	RHS_Cs502	NAT_Hay_H12	RHS_S89	NEA_Kr-d33	-	Qafzeh11
	Mauer	QC_G22	BLZ_026	NEA_Kr-d35	RHS_CN232	-	RHS_CN232
	BLZ_014	NEA_Kr-d33	RHS_Cs498	BLZ_037	RHS_CN236	-	QC_G22
Classif. LDA (97.0%, 100.0%)	AMH (Ppost=0.832)	NEA (Ppost=0.997)	NEA (Ppost=0.827)	AMH (Ppost=1.000)	AMH (Ppost=0.980)	-	NEA (Ppost=0.570)
M2 Cervical OL	QC	Mauer	Ohalo 1	Qafzeh 9	Qafzeh 11	Amud 1	Ehringsdorf G
	Tabun2	NEA_Kr-d86	NAT_Hay_H28	BLZ_014	Qafzeh_15	LaQuina5	NEA_Kr-d86
	NEA_Kr-d10	NEA_Kr-d3	RHS_S4	RHS_140	RHS_S86	RHS_S46	Ehrings_F
	NEA_Kr-d104	BLZ_026	Qafzeh11	RHS_S46	RHS_S4	Qafzeh_15	Tabun2
	NEA_Kr-d2	Ehrings_F	NEA_Kr-d107	RHS_S86	BLZ_014	NEA_Kr-d107	QC_J15
	NEA_Kr-d6	NAT_HayH13	EAR_H298	Qafzeh11	NAT_AM_H55	RHS_S4	Kebara2
Classif. LDA (96.2%, 90.9%)	NEA (Ppost=0.984)	NEA (Ppost=1.000)	NEA (Ppost=0.862)	AMH (Ppost=1.000)	AMH (Ppost=0.997)	NEA (Ppost=0.970)	NEA (Ppost=0.991)
M2 Crown OL	QC	Mauer	Ohalo 1	Qafzeh 9	Qafzeh 11	Amud 1	Ehringsdorf G
	NEA_Kr-d6	NEA_Kr-d104	Qafzeh11	RHS_140	RHS_S86	RHS_S4	NEA_Kr-d86
	RHS_S86	NEA_Kr-d10	NAT_AM_H55	Qafzeh11	NAT_AM_H55	LaQuina5	Mauer
	NEA_Kr-d2	BLZ_026	RHS_S86	NAT_AM_H55	Kebara2	BLZ_026	Qafzeh15
	Kebara2	NEA_Kr-d6	EAR_H298	Kebara2	BLZ_014	Kebara2	NAT_Hay_H28
	Qafzeh11	RHS_S16	BLZ_014	RHS_S86	RHS_S126	BLZ_037	NEA_Kr-d104
Classif. LDA (92.0%, 88.9%)	NEA (Ppost=0.994)	NEA (Ppost=0.968)	AMH (Ppost=1.000)	AMH (Ppost=0.961)	AMH (Ppost=0.982)	NEA (Ppost=0.773)	NEA (Ppost=0.989)
M2 EDJ	QC	Mauer	Ohalo 1	Qafzeh 9	Qafzeh 11	Amud 1	Ehringsdorf G
	NEA_Kr-d3	NAT_HayH13	-	RHS_S16	RHS_S86	-	NEA_Kr-d86
	NEA_Kr-d86	QC_J15	-	BLZ_014	NAT_Hay_H13	-	NEA_Kr-d104
	Ehrings_G	Qafzeh15	-	EAR_H298	BLZ_026	-	NEA_Kr-d6
	NAT_Hay_H13	NEA_Kr-d86	-	RHS_S4	NAT_Hay_H12	-	QC_J15
	BLZ_026	Ehrings_G	-	NAT_AM_H87	NAT_AM_H55	-	NEA_Kr-d10
Classif. LDA (100.0%, 100.0%)	NEA (Ppost=1.000)	AMH (Ppost=1.000)	-	AMH (Ppost=1.000)	AMH (Ppost=1.000)	-	NEA (Ppost=1.000)

contrast to the premolars, the Qesem lower molar is quite large, ranging within the IQR of NEA for all three traits. Mauer M_2 is large too in all aspects, thus in the size range of NEA, while Ehringsdorf M_2 is intermediate between NEA and AMH.

3.2.2. Shape

Differently from size, results for shape are more difficult to interpret. Not all of the nine analyses show a distinct separation between AMH and NEA based on the first two Principal Components (PCs) (Fig. 4B and C. show P_4 EDJ and M_2 EDJ respectively, which represent two extreme examples in terms of degree of separation). Table S1 summarizes a non-parametric MANOVA to test for significant shape differences between AMH and NEA (only specimens of these groups were used). Crown outlines of P_3 and P_4, and EDJ surfaces of P_4 deliver only weak results. All other differences of the permutation tests are highly significant. This, however, does not imply that each individual specimen clusters clearly with its group (see, for instance, NEA_Kr-d26 in Fig. 4B.). We can state that lower P_4 shape is a less powerful data source to reliably distinguish between NEA and AMH, and the same is true for lower premolar crown outlines in general (but cf. Bailey and Lynch, 2005; Gómez-Robles et al., 2008).

While P_3 crown, and P_4 crown and EDJ shape plots deliver generally rather unclear pictures, in the other analyses the Qesem teeth are often found at the fringes of the AMH and NEA shape distributions. Only for P_4 cervical outline and M_2 EDJ surface Qesem is right within the NEA cluster. In the former case, however, Qesem establishes a separate cluster with Mauer and Bilzingsleben that is located at the extreme end of PC1, even beyond the NEA shape trend. The Qesem premolars are generally in the vicinity of the Mauer premolars. The Qesem molar, in contrast, is far apart from Mauer. The oldest material in the sample, Sangiran, is very clearly in the modern human shape distribution (but only P_3s were

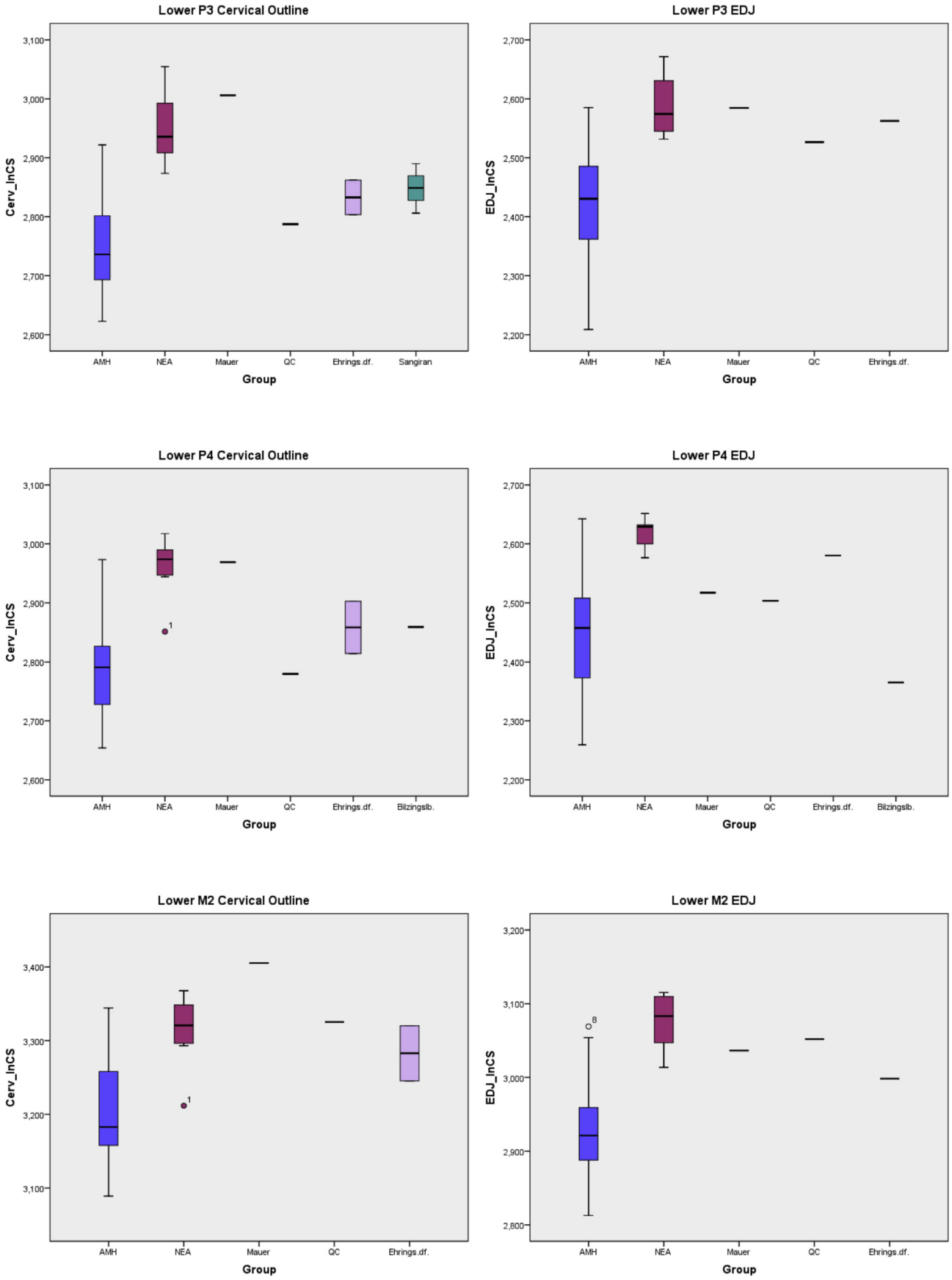

Fig. 3. LN Centroid Size for the three tooth types for cervical outlines and EDJ surface (crown outlines are not plotted here, but results are very similar to cervical outlines). No. 1 = Amud; no. 8 = Qafzeh 9.

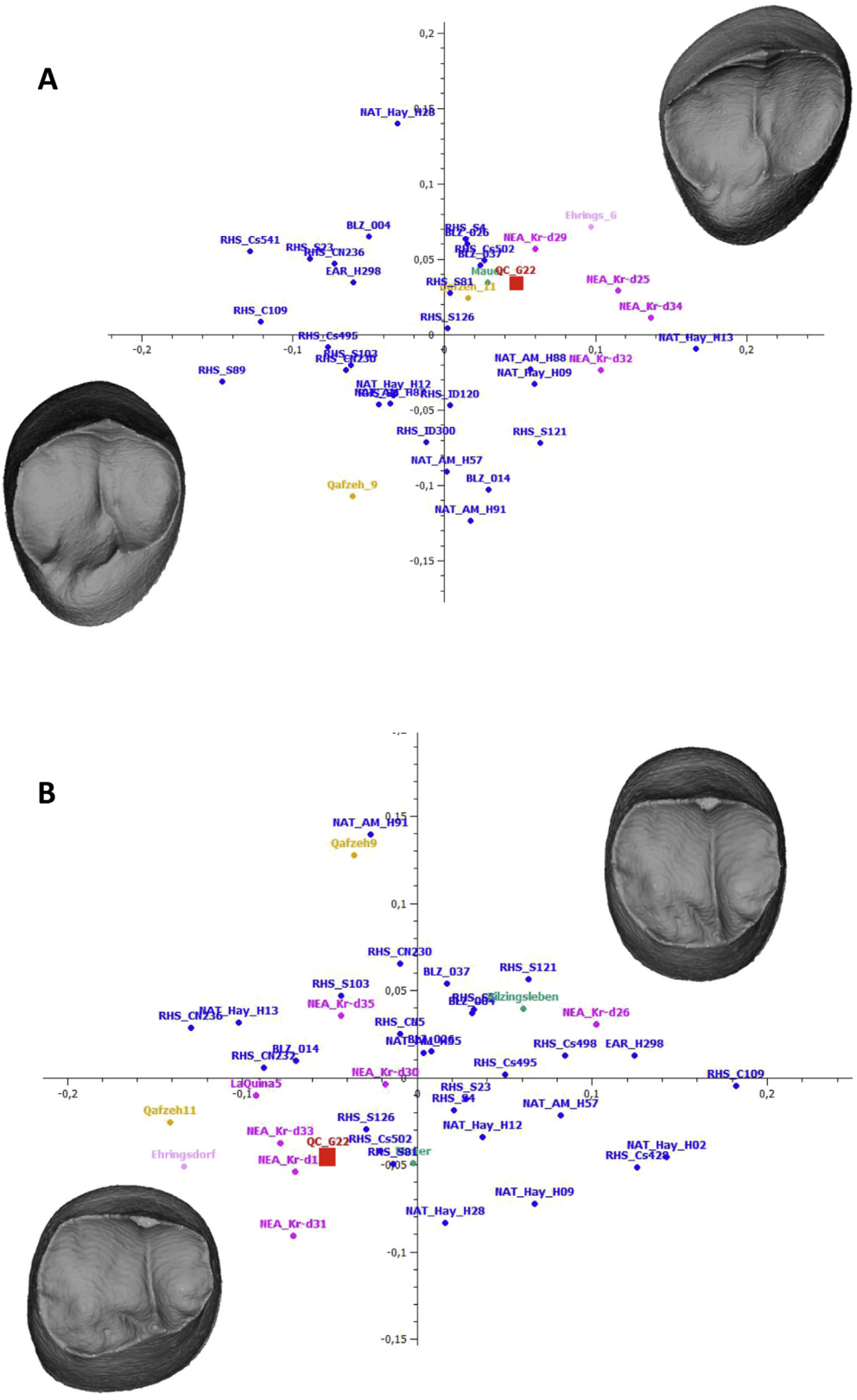

Fig. 4. PCA in shape space. Warped shapes (in each case the surface of a Qesem specimen) for PC −/− and PC+/+ (in panel A. and B.), respectively for PC−/+ and PC +/− (in panel C.) shown. A. P_3 EDJ surface showing a neat but imperfect separation between AMH and NEA. Qesem and Mauer are at the fringes of the two groups. B. P_4 EDJ surface showing a quite weak separation between AMH and NEA (see also NP-MANOVA Table 2). C. M_2 EDJ shape with a perfect separation between AMH and NEA. Note the heart-shaped marginal ridge of Qafzeh 9.

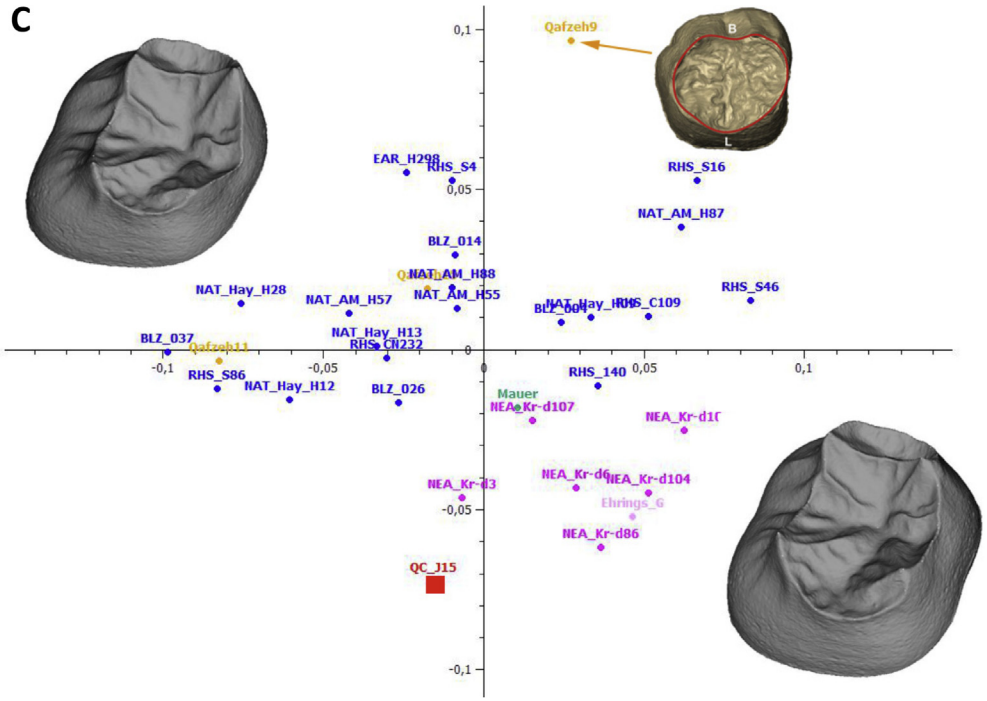

Fig. 4. (*continued*).

available). Ehringsdorf is always near the Neanderthals, Bilzingsleben and Mauer are rather intermediate. These PC plots, however, only capture the situation for the first two PCs, which explain, by definition, most of the variance but curtail the total information available.

The associated shape changes can be visualized by warping the average shape along PC1 and PC2, respectively relevant combinations of them. Starting with P_3 EDJ surface, we can exemplify NEA lower third premolars (Fig. 4A.) as having a more rhomboid and asymmetric silhouette (from occlusal view), and a truncation of the mesiolingual aspect. These observations agree with those made by Gómez-Robles et al., 2008 for *H. heidelbergensis* and *H. neanderthalensis* (including SH) using a different approach (orientated 2D photographs) to study lower P_3 OES. We observe in addition on the EDJ a relatively larger mesial fossa, and low lingual horn tips (the highest elevation of the EDJ underneath an enamel cusp tip). AMH lower third premolars, in contrast to NEA, present an oval and more symmetric silhouette (as do the Sangiran specimens), which is also in agreement with Gomez-Robles and colleagues' findings on the OES (2008), except that they find circular outlines as being typical for *H. sapiens*. On EDJ, we find also a relatively smaller mesial fossa for AMH, but, similarly to NEA and generally differing from lower P_4s, also quite low lingual horn tips. The Qesem third premolar features only a mildly rhomboid and asymmetric silhouette, a fairly truncated mesiolingual portion of the tooth, a large mesial fossa, and a low lingual horn tip. This composition of features places Qesem at the border of the NEA distribution, near Mauer, Qafzeh 11, and modern humans. Qafzeh 9 is very different to Qafzeh 11, and Ehringsdorf G shows the whole set of NEA features in an extreme form.

Looking at P_4 EDJ surface (Fig. 4B) we can describe NEA lower fourth premolars as having a more subequal (i.e., a relatively shorter B/L diameter) but asymmetric silhouette owing to a mesiolingual truncation of the lingual lobe (also observed by Bailey and Lynch (2005), as well as by Martinón-Torres et al. (2006) on the OES, using again 2D photographic approaches). In addition, we find on the EDJ a markedly smaller mesial fossa (which seems to be associated with the mesiolingual truncation), and a more equal height of buccal and lingual horn tips (the latter still being a bit lower than the buccal one). AMH lower fourth premolars show quite a lot of variation but the trend for shape can be described as an almost perfect oval (i.e., a relatively elongated B/L diameter) and symmetric silhouette, which confirms the OES findings of Bailey and Lynch (2005) and Martinón-Torres et al. (2006). AMH have rather a larger mesial fossa, and a relatively low lingual horn tip. The early anatomical modern humans Qafzeh 9 and 11 are, again, quite different from each other with regard to the silhouette (Qafzeh 9 imperfectly oval, Qafzeh 11 subequal with mesiolingual truncation), but both feature small mesial fossae. Bilzingsleben is almost oval in shape and within the modern human distribution. Mauer, against it, is much less oval. Qesem has a moderately relative B/L length, a small mesial fossa, a relatively high lingual horn tip – compared to the buccal one, and definitely a mesiolingual truncation of the lingual lobe. Together with Mauer, it is found at the border of the distributions of NEA and AMH. Ehringsdorf G is close to Qafzeh 11 and again on the extreme of the NEA cluster, thus showing all features mentioned above in an extreme expression.

The shape of the M_2 EDJ surface (Fig. 4C) of NEA and also Qesem is characterized by a more rectangular silhouette that is mesiodistally larger, has a buccolingually wider talonid, and relatively higher buccal horn tips (protoconid and hypoconid). This is contrasting with AMH which features a less elongated silhouette, exhibiting a conspicuous convexity of the lingual marginal ridge between the metaconid and entoconid. In extreme cases, such as Qafzeh 9, the marginal ridge can adopt a heart-shaped rather than a rectangular outline (Fig. 4C). The talonid appears buccolingually narrower due to this convexity in the middle of the tooth on the one hand, and a more inwardly positioned entoconid on the other hand. Generally, the entoconid is reduced, and the hypoconid and entoconid are placed slightly more distally. Qesem also exhibits this more distal placement of the distal cusps but lacks the marked

convexity of the lingual margin, the narrow talonid, and particularly the inwardly positioned entoconid. Alltogether, it is quite NEA-shaped and, like Ehringsdorf G, clearly in their shape distribution. On the other hand, its hypoconulid is absent. Four cusped M_2s were not detected in Neanderthals and other archaic hominins in a study by Bailey (2006). The two Qafzeh specimens are not close to each other, still they plot within the AMH cluster, far from NEA.

The PLS analysis ($n = 32$) shows how P_3 and P_4 EDJs covary. The plot for the left and right first singular warps (percentage of total squared covariance for pair 1 = 59.1%, pairwise correlation between singular warp 1 left and singular warp 1 right $r_1 = 0.637$), and the correspondent covariation between P_3 and P_4 is visualized in Fig. 5. They can be understood as shape changes in P_3 that best explain shape changes in P_4, and vice versa. The distribution of the sample is elliptical, running from the left lower −/− quadrant to the right upper +/+ quadrant. Although there were only very few NEA specimens qualifying for this analysis, the shape changes look very similar to the results of the isolated analyses for P_3 and P_4. That means rhomboid and asymmetric P_3 silhouette showing a truncation of the mesiolingual aspect, a small P_4 mesial fossa, and also a mesiolingual truncation of the lingual P_4 lobe on the side of NEA. On the opposite side of AMH, there are more oval and symmetric P_3 and P_4 silhouettes with relatively smaller P_3 and larger P_4 mesial fossae. These matching trends in lower premolars and the fairly high correlation between singular warps left and right are a hint on functional constraints that are likely behind a concerted shape change during evolutionary development, rather than random fluctuations. However, there is not much known about these relationships and we will have to await further studies on whole dentitions. The two Qafzeh individuals are again quite divergent – Qafzeh 9 perfectly in the AMH distribution, and Qafzeh 11 on the NEA end.

In addition to these relative warps and PLS analysis we looked at other statistics to interpret the relations between groups and the tentative associations of individual specimens. Firstly, we calculated the five nearest neighbors of Qesem and some other individuals for all three traits and tooth types in shape space (Table 2). These data are based on the full Procrustes distances, and thus have not the same information content as the first two PCs. Secondly, we performed linear discriminant analyses (LDA) using the individual

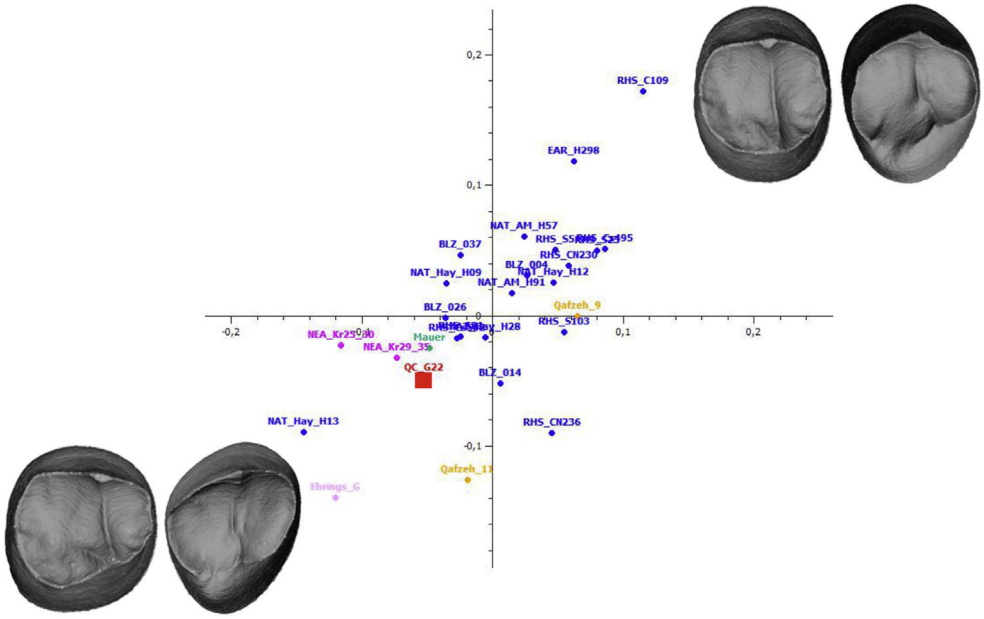

Fig. 5. PLS of EDJ shapes for P_3 (right of the each pair) and P_4 (left of each pair).

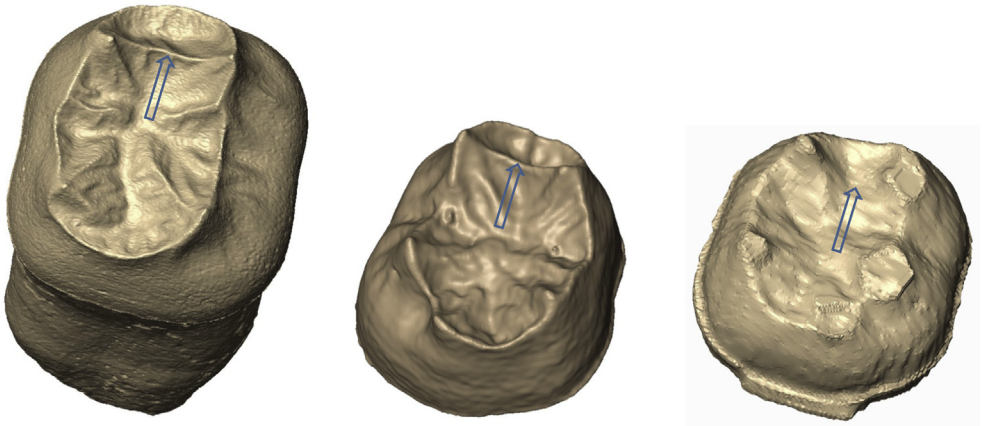

Fig. 6. The M_2 trigonid crest in Qesem (left), Ehringsdorf G (middle), and Mauer (right). Not to scale.

scores of the first ten PCs in shape space which explain between 87.3% and 98.8% of the total variance. Only specimens that we clearly assigned to either AMH or NEA (see Table 1) were used to establish the two groups. Early-to Mid-Pleistocene fossils were not part of these groups. Table 2 provides the percentage of correctly classified AMH and NEA specimens in the linear discriminant analyses, and the predicted group memberships for all Early-to Late-Pleistocene specimens, as well as the probabilities for this classification (Ppost). The pictures drawn by the five nearest neighbors on the one hand, and the linear discriminant analyses on the other, can be consistent, but do not have to be. This is because LDA is a multivariate approach considering the covariance structures of the groups, whereas Procrustes distance does not. In particular, if the difference between the established groups in LDA is heavily weighted on high-numbered PCs (which it often is), then the discrimination will likely deviate from the simple optimization based on Procrustes distance. In other words, LDA might focus on small scale features represented in, e.g. PC6 or PC9, and Procrustes distance is an added distance across the full multidimensional space.

We included also the Late-Pleistocene hominins Amud 1, Qafzeh 9, Qafzeh 11, and Ohalo 1 into this comparison, although their taxonomic affiliation to NEA, respectively to AMH, is out of question from our point of view. The reason was to see how they would perform in this approach. Sangiran, Bilzingsleben E6, and Ohalo 1 just appear in one tooth type because only this material was available. Some of the EDJ analyses (also for Amud 1) had to be left out because the μCT scans, respectively the preservational status, did not allow for inclusion.

Out of the nine Early-, Mid-, and Late-Pleistocene specimens, three show an entirely unambiguous picture. Notably these three are not from the Mid-Pleistocene. Sangiran (in fact all three teeth in the sample, but only S7-25 shown in Table 2), Qafzeh 9, and Qafzeh 11 have only or almost only AMH as nearest neighbors, and the LDA puts them in this group in *all* analyses. This, of course, does not mean that Sangiran is modern human, but the outline shapes of these Early-Pleistocene premolars are virtually indistinguishable from moderns. This could be a hint on a plesiomorphic trait, but additional Early-Pleistocene material would be needed to support this notion. Interestingly, Qafzeh 9 and Qafzeh 11 show a quite high frequency of nearest neighbors from the Levantine Natufian and Bedouin sample, sometimes also affinities to a Neanderthal. Although the two Qafzeh specimens are not quite similar in shape, our discriminant analysis has no problem assigning them both unequivocally to the modern human group in all cases. A closer relationship of Qafzeh 9 or Qafzeh 11 to the Qesem material is not inferable from these data.

The other two Late-Pleistocene specimens do not lead to unequivocal affinities, but are largely consistent with their current classification. Ohalo 1 is only represented with M_2 outlines here. Its nearest neighbors are almost exclusively modern humans, but the LDA is indecisive with one classification in NEA and one in AMH. Amud 1 is represented by outlines only since the EDJ is too much affected by heavy wear. It has almost no nearest neighbor from the Mid-Pleistocene (except Ehringsdorf G for P_4 crown outline), but its premolar outlines are quite near modern humans with a noticeable high frequency of Levantine Natufians and Bedouins. The discriminant analyses, however, group it five out of six times with NEA.

The Mid-Pleistocene material is more or less unambiguous only with regard to Ehringsdorf. The predominant signal is that its nearest shape neighbors are mainly Neanderthals (and in some cases also Qesem and Mauer), and nine out of nine LDA results led to a grouping with NEA. This is strongly supporting the view that Ehringsdorf represents indeed an early form of Neanderthals, one that has not yet developed the full suite of NEA traits (cf. beginning Neanderthal distinctiveness with step 3 in Harvati et al., 2010).

However, except Ehringsdorf, the other three Mid-Pleistocene fossils produce a quite heterogenous picture. Mauer and Qesem are represented by all three teeth, Bilzingsleben only by one premolar. All are intermediate in shape, their nearest neighbors switch between AMH, NEA, and between each other. The LDA places each of them exactly in one third of traits into AMH (one out of three for Bilzingsleben, three out of nine for Mauer and Qesem) – though sometimes with a quite low posterior probability (Ppost) – and in two thirds into NEA. It is worth noting that the base of the P_4 (cervical outline) particularly features a more Neanderthal-like shape and is quite similar among these three Mid-Pleistocene specimens. The crown outline is much more modern-like. The Qesem M_2 cervical outline is also overwhelmingly NEA-like.

3.2.3. Form

If we merge shape and size, we observe highly significant differences between our two groups AMH and NEA in *each* trait for *each* tooth type (see Table S1). Fig. S3 shows two examples in this form space. In each of the six plots for the premolars, Qesem lies within the AMH cluster or near the border between AMH/NEA because of the small size, which is the dominating factor for PC1. For the molar, this picture is reversed, i.e. Qesem is always located within the NEA distribution. Yet, also Mauer, Qafzeh, and one Sangiran specimen are found there, again due to their big size. Evolutionary allometry (across phylogenetically related species) is rather low, i.e. only 4.5% of P_3, 8.7% of P_4, and 11.5% of M_2 EDJ shape variance can be explained by lnCS. Other authors have suggested a negligible influence of size on shape in lower hominin premolars (Bailey and Lynch, 2005). Martinón-Torres et al. (2006) found a similar allometry (7.5%) than we did for P_4s, and Gómez-Robles et al. (2008) calculated a higher 17.3% allometric effect for lower P_3s, however, both in samples that comprised hominin taxa from Australopithecines to modern humans, thus embracing a much greater variation in shape and size than our study. This means that allometry is playing a minor role in Mid-to Late-Pleistocene *Homo* premolars. A larger sample of geographically very diverse recent humans also confirmed values of allometry around 5% for lower premolars (Krenn, 2015). Since size and shape of the lower postcanine dentition are rather loosely connected in the period from the Mid-Pleistocene to the Holocene, we put less weight on form results in the interpretation and rather focus on size and shape results separately.

3.2.4. Qualitative results

The virtual representation of the segmented EDJ allows observing qualitative characteristics too. On the Qesem molar EDJ (Fig. 6 left), we observe a strong “grade 3” trigonid crest (Bailey et al., 2011), described as being the most frequent grade in NEA, but completely absent in a sample of modern humans. Ehringsdorf G features exactly the same type of middle trigonid crest (see Fig. 6 middle). Mauer (see Fig. 6 right) and Qafzeh 9, in contrast, present only weak distal crests, and Jebel Irhoud 3 lacks it completely, according to the aforementioned authors. A middle trigonid crest was also observed on the EDJ of the Tighenif material (Zanolli and Mazurier, 2013). In Qesem and Ehringsdorf, the crest originates at the protoconid and metaconid and connects them in a straight line. A discontinuous distal trigonid crest is visible. According to Martínez de Pinillos et al. (2014), the Qesem trigonid crest on the EDJ would correspond to a “Type 12 continuous middle trigonid crest with discontinuous distal trigonid crest”. Such a configuration never appeared in their sample of M_2s in *H. sapiens* and NEA, but in 18.2% of the SH sample. According to the same author's scheme,

Qesem features a "Type A" trigonid crest on the OES, which has a frequency of 87.5% in NEA, 100% in SH, but only 25% in *H. sapiens*. Trigonid crests were also observed on the OES in the Sangiran sample (Kaifu et al., 2005), and in *Homo antecessor* (Martinón-Torres et al., 2007). Another qualitative observation, namely the absence of a hypoconulid in our Qesem lower M_2, was shown to have a frequency of zero in a sample of 39 Neanderthals in a study by Bailey (2006). Gómez-Robles et al. (2015) point out the marked tendency to distal reductions in later *Homo* species (including both, NEA and AMH), compared to Australopithecines and early *Homo*.

There was an additional tooth found at Qesem cave, a lower third molar (M_3-Q13), which is not included in this geometric morphometric analysis because we consider the intra-species shape variability of M_3s as generally too high to use it successfully in our approach (but see Bailey (2006) for a different opinion, using a different approach, and Zanolli and Mazurier (2013)). M_3-Q13 is described in this volume in detail (Hershkovitz et al., 2016). The tooth comes from a layer dated to >300 ka and is thus of similar chronological age as the other mandibulary teeth in this study. A strongly expressed trigonid crest is visible on the OES. Looking at the segmented data of the EDJ, we also find a markedly expressed middle trigonid crest. It is continuously running from protoconid to metaconid in a straight line. Its height dips slightly more towards the midline than those crests of the above mentioned M_2s of Qesem or Ehringsdorf G, but we would still see it in correspondence with a grade 3 in Bailey et al. (2011) scoring system (see image in Hershkovitz et al. (2016)).

4. Discussion

Qesem Cave, with regard to hominins, delivered only isolated teeth. Not one single tooth type in the record is represented by more than one specimen, and they come from different layers that might comprise a period of roughly 150 ka. To reduce some of these difficulties, we focused on the three lower postcanine teeth in this study because they represent some of the oldest material from Qesem (which reduces the time difference to roughly 50 ka), and two of them (P_3 & P_4) belonged to the same individual. Concordant results from these two could at least show morphological tendencies clearer than results from just one specimen; nevertheless, the population variation covered here remains the smallest possible random snapshot.

Anatomically modern humans and Neanderthals represent two hominin demes that emerged during the late Mid-Pleistocene and survived until the upper Late-Pleistocene, before Neanderthals went extinct. Morphologically, the skeleton and the dentition developed numerous characteristic differences (e.g., Santa Luca, 1978; Stringer and Andrews, 1988; Schwartz and Tattersall, 1996; Hublin, 1998; Ponce de Leon and Zollikofer, 2001; Lieberman et al., 2002; Bruner et al., 2003; Harvati, 2003; Bailey and Lynch, 2005; Bailey, 2006; Bastir et al., 2008, 2010; Gunz et al., 2010; Harvati et al., 2010; Gómez-Robles et al., 2011; Gómez-Olivencia et al., 2013; Martinón-Torres et al., 2013; Bastir et al., 2015). Our quantitative approach using the EDJ and cervical and crown outlines of three types of teeth is able to differentiate between AMH and NEA quite well. 24 out of the 27 analyses led to highly significant shape or form differences between those groups. The discriminant analyses were able to correctly classify members of these two groups in 87.5–100%. With regard to the Early-to Mid-Pleistocene specimens, the morphology of the Qesem teeth can be characterized as intermediate between NEA and AMH. This statement is also applying to other Mid-Pleistocene fossils in the sample such as Mauer and Bilzingsleben. It is worth noting that our study uses 3D data and includes the internal morphology. This allows a detailed analysis of the tooth geometry but reduces the available sample. Our approach delivers phenetic results (statements about similarity and differences, not phylogenetic relationships) and is mainly based on material that appeared chronologically *later* than Qesem, Mauer, and Bilzingsleben. Although all these three specimens feature similarities to Neanderthals to some extent, for a cladistic approach it would be necessary to know the ancestral state *before* Qesem, Mauer, and Bilzingsleben. There are two requirements that we cannot meet for one or two instances in our study: 1) identification of material that is ancestral to our Mid-Pleistocene sample, and 2) access to high-resolution data from this material.

The picture that can be drawn is yet more differentiated than only confirming an intermediate morphology. Regarding shape, the Qesem molar is quite similar to NEA (more than Mauer). The strong expression of the mid-trigonid crest would emphasize also similarity to NEA. However, interpretation of this qualitative trait needs to be cautious since there are other cases such as Sangiran (Kaifu et al., 2005), *Homo antecessor* (Martinón-Torres et al., 2007), or Tighenif (Zanolli and Mazurier, 2013) that feature a mid-trigonid crest much earlier. The Qesem premolars are as intermediate between NEA and AMH in shape as those from Mauer and Bilzingsleben. However, in terms of size Qesem premolars are quite modern-like, outside the range of NEA, and smaller than Mauer. The Qesem molar in contrast is large (almost outside the range of AMH). The three much older Sangiran teeth do not show ambiguity and are quite similar to AMH (but only P_3 outlines could be tested). Ehringsdorf, on the opposite, is by all means more developed into the NEA direction than any other Mid-Pleistocene specimen in our sample. Yet, it is also chronologically younger than those.

In summary, there are features present in the Mid-Pleistocene sample that are characteristic for Neanderthal morphology. These features can be metrically used to distinguish between the later NEA and AMH. They are usually expressed in Qesem more moderately than in NEA, while Ehringsdorf shows them very clearly. Also Mauer, and in some cases Bilzingsleben, carry some of these features. Mauer, however, was recently dated to ~ 609 ka (Wagner et al., 2010). Geneticists estimate the separation leading to Neanderthals and anatomically modern humans around 589–270 ka (see introduction). Thus those traits could have been already present before the calculated split which raises two questions: 1) How likely is an evolutionary scenario proposing a split and a more or less linear development towards the two hominin demes NEA and AMH without considering complex population dynamics during the Mid-Pleistocene (see Dennell et al., 2011)? 2) Could the genetic models be wrong, hence, could the separation have occurred much earlier? The SH sample falls well into the earlier half of the estimated period (427 ka) and shows that many Neanderthal traits were already present at this time in Western Europe. In some dental classes the SH hominins show even more derived morphologies than Neanderthals (Gómez-Robles et al., 2015). Our results are basically in agreement with the view expressed by Gómez-Robles et al. (2013) who found Neanderthal dental affinities in all late Early- and Mid-Pleistocene taxa from Europe and speculated about the existence of a separate European clade with Neanderthal affinities since at least 1 Million years. However, their study did not include non-European Mid-Pleistocene material.

Since so many basic questions of NEA and AMH development are in dubio (probably more than scholars thought in the past decades), it seems unrealistic to definitely assess the affiliation of the Qesem sample, which is only known from a few isolated teeth. What can be stated is that a Mid-Pleistocene hominin population was present in Southwestern Asia that shows some Neanderthal affinities, probably more than Mauer and

Bilzingsleben, but less than Ehringsdorf. We cannot exclude that Qesem, Mauer, and Bilzingsleben could be members of one taxon, which then would make it incidentally very unlikely that they represent Denisovans. Qesem could also be a local phenomenon which raises an interesting question: did these people leave traces in later populations? Some nearest shape neighbours of Qesem were Qafzeh 9, Qafzeh 11, Amud 1, Kebara 2, and Tabun 2. In Mauer's nearest neighbourhood list there appear two of the Qafzeh specimens, but no Levantine Neanderthals. Bilzingsleben has no Pleistocene Levantine neighbours other than Qesem.

Evolutionary changes can affect both the shape of a structure, as well as its size. Gould (1977, p 234f) and other researchers before and after him argued about this. The basal insight was that ontogeny and evolution are interrelated because changes in the developmental processes are producing morphological variation which in turn is the basis for evolutionary processes such as natural selection. In this event, growth (the increase in size) and development (any change in shape during ontogeny) can be dissociated, respectively can be affected by different factors. The Qesem premolars are intermediate in shape between NEA and AMH, their size is quite small, i.e. in the middle to lower range of AMH. The divergence of shape and size is also remarkable looking at other Levantine cases, for instance, Qafzeh 9 which often appears within a cluster of NEA in form space due to its very large size, at the same time featuring definitely a modern shape. Qafzeh 11 on the other hand is quite small and mostly in the range of AMH for shape. Amud 1, described as featuring a more progressive morphology (Suzuki and Takai, 1970), is a microdont Neanderthal (Trinkaus, 1984). It comes close or is in the cluster of AMH in form space due to this small tooth size in the range of AMH. The fact that we find such cases in the fossil record calls for caution, especially the large size range of the Qafzeh population.

Diverging trends for shape and size of dental elements in our small sample could reflect just random variation. However, one actual factor allowing for size reduction without losing fitness was established at least around the time of our Qesem population. Cooking changes the physical properties of food quite radically, and dramatically reduces the work of the dentition and masticatory apparatus (Lucas, 2004). Some authors claimed a very early appearance of cooking, even in the Early-Pleistocene (e.g. Wrangham, 2009), while others suggested that ubiquitous cooking, at least in Eurasia, started later around 400–300,000 years ago (Roebroeks and Villa, 2011; Shahack-Gross et al., 2014), and the diet in the Levant might have changed around the same time (Ben-Dor et al., 2011). Dental dimensions remained relatively stable in *H. erectus* populations, but declined gradually since about 300 ka (Lucas, 2004). Changing size along an evolutionary pathway is not necessarily coupled with changing shape. Martinón-Torres et al. (2013) found shape variables of the SH upper M^1s to match the *H. neanderthalensis* pattern, while size related measures were similar to *H. sapiens*. Studying cusp areas, Quam et al. (2009) found a general size reduction of upper M^1s in the genus *Homo*, and shifts between relative cusp sizes. Bermudez de Castro et al. (1999) suggested an imbalance of the sizes for I_1-P_3 on the one hand, and P_4-M_3 on the other for *H. heidelbergensis* which would point to different evolutionary trends for anterior and posterior dentitions (they suggested to place the boundary between anterior and posterior dentition after P_3 rather than after C). We cannot confirm this different pattern for P_3 and P_4 of Qesem, but their results remind us to keep dissociated size developments in mind. The notable size-shape pattern of the Qesem teeth suggests three different hypotheses:

- H^1: The different patterns seen in the premolars and in the molar is due to mere individual variation and has no further meaning.
- H^2: The premolars and the molar originate from different populations inhabiting Qesem Cave at different times (corresponding roughly to a maximum difference of 50 ka).
- H^3: The premolars and the molar are from the same population and represent a typical pattern. Premolars show a clear tendency towards size reduction, at the same time featuring an intermediate shape between NEA and AMH. Molars are closer to NEA in size and shape.

The random case formulated in H^1 cannot be excluded, as in all other cases of isolated fossil findings.

H^2 does not seem to be likely since culturally [concerning the habitual use of fire; lithic economy, technology, typology and recycling patterns; faunal composition and hunting and butchering patterns (Karkanas et al., 2007; Stiner et al., 2009, 2011; Shimelmitz et al., 2011, 2016; Shahack-Gross et al., 2014; Blasco et al., 2014; Parush et al., 2015)] the Qesem Cave context provides no reason to support the hypothesis of two different populations. However, this line of argumentation is based on the assumption that evolutionary changes of human body parts (teeth in this case) would “instantly” (i.e., within several tens of thousands of years) result in a recognizable behavioural change, which is certainly problematic. Still, if we assume that the chronologically younger molar originates from a Qesem population that was more derived towards Neanderthals, we still have to explain the peculiar size-shape pattern of the premolars.

H^3 gains credit if we are willing to accept the rejection of H^1 and H^2. We are facing a scenario suggesting dissociating size and shape trends in the Mid-Pleistocene in the Levant. This exemplifies a pattern of form in postcanine dentition that is neither NEA, nor AMH, or another Mid-Pleistocene population as it was represented in our sample. As the low amount of allometry (5–12%) suggests, size and shape are not strongly related to each other, at least for premolars and molars.

5. Conclusions

The two lower premolars and the lower molar investigated in this study are among the oldest material (>300 ka) recovered so far from Qesem Cave. Yet, the premolars and the molar were not found in the same strata, therefore there could still be considerable time difference between them. Our geometric morphometric approach is able to distinguish quite well between dental specimens from two Pleistocene hominin demes, AMH and NEA. It also confirms in general the intermediate morphology of Mid-Pleistocene specimens, respectively a closer similarity of some with regard to AMH or NEA. The Qesem premolars display such an intermediate shape between NEA and AMH, but their size is definitely modern-like. The Qesem molar features a shape and size nearer to NEA. This suggests three different hypotheses for explanation. One of them advocates a dissociation of size and shape in premolars, and molars that are morphologically closer to Neanderthals than premolars.

With the current data, we cannot assign the Qesem teeth to any existing taxon nor exclude that it is a new taxon appearing in the Levant. Qesem shows Neanderthal-affinities, but it is definitely not as close to Neanderthals as Ehringsdorf. Moreover, the reduced size of premolars would put Qesem rather closer to AMH, but the molar morphology is again suggesting differently. Whether Qesem was a local phenomenon or reflects a typical pattern of *Homo* phylogenetic development in Eurasia cannot be decided.

The Qesem lower premolars and molars are morphologically characterized quite comprehensively with this study. For a definite taxonomic assessment of the Qesem population, however, more complete specimens from the cave are needed, as well as better models for the evolution of *Homo* in the Mid-Pleistocene in general.

Acknowledgements

We thank Martin Dockner for support during µCT scanning, Roman Ginner for taking photographs, and Vivian Slon, Hila May, and Aviad Agam for helping with the transport of the Israeli material. We thank the Tel Aviv University Anthropological Collection, the Croatian Natural History Museum in Zagreb, the Muséum National d'Histoire Naturelle in Paris, AST-RX - Plateau technique d'imagerie tomographique RX the Ruprecht Karls Universität Heidelberg, the Max-Planck Institute Leipzig, the Thüringisches Landesamt für Denkmalpflege und Archäologie Weimar, and NESPOS for access to fossils, respectively for scanning fossils. We are grateful to Maria Martinón-Torrez, José Maria Bermúdez de Castro, Tim Schüler, Inga Stolbovaya, and Rudolf Slavicek for discussion and comments. This research was supported by the Department of Anthropology at University of Vienna, A.E.R.S. Dental Medicine Organisations GmbH, Vienna, Austria (FA547014), and the Siegfried Ludwig - Rudolf Slavicek Stipendienstiftung (FA547016). The anthropological study of the Qesem hominids is supported by the Dan David Foundation.

Appendix A. Supplementary data

Supplementary data related to this article can be found at http://dx.doi.org/10.1016/j.quaint.2015.10.027.

References

Arnold, L.J., Demuro, M., Parés, J.M., Arsuaga, J.L., Aranburu, A., Bermúdez de Castro, J.M., Carbonell, E., 2014. Luminescence dating and palaeomagnetic age constraint on hominins from Sima de los Huesos, Atapuerca, Spain. Journal of Human Evolution 67, 85–107.

Bailey, S., 2006. Beyond shovel-shaped incisors: Neandertal dental morphology in a comparative context. Periodicum Biologorum 108, 253–267.

Bailey, S.E., Lynch, J.M., 2005. Diagnostic differences in mandibular P4 shape between neandertals and anatomically modern humans. American Journal of Physical Anthropology 126, 268–277.

Bailey, S.E., Skinner, M.M., Hublin, J.J., 2011. What lies beneath? An evaluation of lower molar trigonid crest patterns based on both dentine and enamel expression. American Journal of Physical Anthropology 145 (4), 505–518.

Barkai, R., Gopher, 2013. Cultural and Biological Transformations in the Middle Pleistocene Levant: a View from Qesem Cave, Israel. The Replacement of Neanderthals by Modern Humans series ('RNMH series'). Springer, pp. 115–137.

Barkai, R., Lemorini, C., Shimelmitz, R., Lev, Z., Stiner, M.C., Gopher, A., 2009. A blade for all seasons? Making and using Amudian blades at Qesem Cave, Israel. Human Evolution 24 (1), 57–75.

Bastir, M., Rosas, A., Lieberman, D.E., O'Higgins, P., 2008. Middle cranial fossa anatomy and the origin of modern humans. Anatomical Record 291, 130–140.

Bastir, M., Rosas, A., Stringer, C., Cuetara, J.M., Kruszynski, R., Weber, G.W., Ross, C.F., Ravosa, M.J., 2010. Effects of brain and facial size on basicranial form in human and primate evolution. Journal of Human Evolution 58, 424–431.

Bastir, M., García-Martínez, D., Estalrrich, A., García-Tabernero, A., Huguet, R., Ríos, L., Barash, A., Recheis, W., de la Rasilla, M., Rosas, A., 2015. The relevance of the first ribs of the El Sidrón site (Asturias, Spain) for the understanding of the Neandertal thorax. Journal of Human Evolution 80, 64–73.

Ben-Dor, M., Gopher, A., Hershkovitz, I., Barkai, R., 2011. Man the fat hunter: the demise of homo erectus and the emergence of a new hominin lineage in the middle pleistocene (ca. 400 kyr) Levant. PLoS One 6.

Benazzi, S., Fornai, C., Buti, L., Toussaint, M., Mallegni, F., Ricci, S., Gruppioni, G., Weber, G.W., Condemi, S., Ronchitelli, A., 2012. Cervical and crown outline analysis of worn Neanderthal and modern human lower second deciduous molars. American Journal of Physical Anthropology 149, 537–546.

Bermudez de Castro, J.M., Rosas, A., Nicolas, M.E., 1999. Dental remains from Atapuerca-TD6 (Gran Dolina site, Burgos, Spain). Journal of Human Evolution 37, 523–566.

Blasco, R., Rosell, J., Gopher, A., Barkai, R., 2014. Subsistence economy and social life: a zooarchaeological view from the 300 kya central hearth at Qesem Cave, Israel. Journal of Anthropological Archaeology 35, 248–268.

Bookstein, F.L., 1978. The Measurement of Biological Shape and Shape Change. In: Lecture Notes in Biomathematics, vol. 24. Springer-Verlag, New York.

Bookstein, F.L., 1989. Principal warps: thin plate splines and the decomposition of deformations. IEEE Trans. Pattern Anal. Machine Intelligence 11, 567–585.

Bookstein, F.L., 1991. Morphometric Tools for Landmark Data: Geometry and Biology [Orange Book]. Cambridge University Press, Cambridge, New York.

Bruner, E., Manzi, G., Arsuaga, J.L., 2003. Encephalization and allometric trajectories in the genus Homo: evidence from the Neandertal and modern lineages. Proceedings of the National Academy of Sciences of the United States of America 100, 15335–15340.

Buck, L.T., Stringer, C.B., 2014. Homo heidelbergensis. Current Biology 24, R214–R215.

Dennell, R.W., Martinón-Torres, M., Bermúdez de Castro, J.M., 2011. Hominin variability, climatic instability and population demography in Middle Pleistocene Europe. Quaternary Science Reviews 30, 1511–1524.

Eller, E., Hawks, J., Relethford, J.H., 2004. Local extinction and recolonization, species effective population size, and modern human origins. Human Biology 76, 689–709.

Endicott, P., Ho, S.Y.W., Stringer, C., 2010. Using genetic evidence to evaluate four palaeoanthropological hypotheses for the timing of Neanderthal and modern human origins. Journal of Human Evolution 59, 87–95.

Gómez-Olivencia, A., Been, E., Arsuaga, J.L., Stock, J.T., 2013. The Neandertal vertebral column 1: the cervical spine. Journal of Human Evolution 64, 608–630.

Gómez-Robles, A., Martinón-Torres, M., Bermúdez de Castro, J.M., Prado, L., Sarmiento, S., Arsuaga, J.L., 2008. Geometric morphometric analysis of the crown morphology of the lower first premolar of hominins, with special attention to Pleistocene Homo. Journal of Human Evolution 55, 627–638.

Gómez-Robles, A., Martinón-Torres, M., Bermúdez de Castro, J.M., Prado-Simón, L., Arsuaga, J.L., 2011. A geometric morphometric analysis of hominin upper premolars. Shape variation and morphological integration. Journal of Human Evolution 61, 688–702.

Gómez-Robles, A., De Castro, J.M.B., Arsuaga, J.L., Carbonell, E., Polly, P.D., 2013. No known hominin species matches the expected dental morphology of the last common ancestor of Neanderthals and modern humans. Proceedings of the National Academy of Sciences of the United States of America 110, 18196–18201.

Gómez-Robles, A., Bermúdez de Castro, J.M., Martinón-Torres, M., Prado-Simón, L., Arsuaga, J.L., 2015. A geometric morphometric analysis of hominin lower molars: evolutionary implications and overview of postcanine dental variation. Journal of Human Evolution 82, 34–50.

Gopher, A., Ayalon, A., Bar-Matthews, M., Barkai, R., Frumkin, A., Karkanas, P., Shahack-Gross, R., 2010. The chronology of the late Lower Paleolithic in the Levant based on U-Th ages of speleothems from Qesem Cave, Israel. Quaternary Geochronology 5 (6), 644–656.

Gould, S.J., 1977. Ontogeny and Phylogeny. Belknap Press of Harvard University Press, Cambridge, MA.

Gower, J.C., 1975. Generalized procrustes analysis. Psychometrika 40, 33–51.

Green, R.E., Krause, J., Briggs, A.W., Maricic, T., Stenzel, U., Kircher, M., Patterson, N., Li, H., Zhai, W., Fritz, M.H.Y., Hansen, N.F., Durand, E.Y., Malaspinas, A.S., Jensen, J.D., Marques-Bonet, T., Alkan, C., Prüfer, K., Meyer, M., Burbano, H.A., Good, J.M., Schultz, R., Aximu-Petri, A., Butthof, A., Höber, B., Höffner, B., Siegemund, M., Weihmann, A., Nusbaum, C., Lander, E.S., Russ, C., Novod, N., Affourtit, J., Egholm, M., Verna, C., Rudan, P., Brajkovic, D., Kucan, Ž., Gušic, I., Doronichev, V.B., Golovanova, L.V., Lalueza-Fox, C., De La Rasilla, M., Fortea, J., Rosas, A., Schmitz, R.W., Johnson, P.L.F., Eichler, E.E., Falush, D., Birney, E., Mullikin, J.C., Slatkin, M., Nielsen, R., Kelso, J., Lachmann, M., Reich, D., Pääbo, S., 2010. A draft sequence of the neandertal genome. Science 328, 710–722.

Grün, R., Stringer, C., 2000. Tabun revisited: revised ESR chronology and new ESR and U-series analyses of dental material from Tabun C1. Journal of Human Evolution 39, 601–612.

Grün, R., Schwarcz, H.P., Ford, D.C., Hentzsch, B., 1988. ESR dating of spring deposited travertines. Quaternary Science Reviews 7, 429–432.

Gunz, P., Mitteroecker, P., 2013. Semilandmarks: a method for quantifying curves and surfaces. Hystrix 24.

Gunz, P., Mitteroecker, P., Bookstein, F.L., 2005. Semilandmarks in three dimensions. In: Slice, D.E. (Ed.), Modern Morphometrics in Physical Anthropology. Kluwer Press, New York, pp. 73–98.

Gunz, P., Neubauer, S., Maureille, B., Hublin, J.J., 2010. Brain development after birth differs between Neanderthals and modern humans. Current Biology 20, R921–R922.

Hammer, O., Harper, D.A.T., Ryan, P.D., 2001. PAST: Paleontological statistics software package for education and data analysis. Palaeontologia Electronica 4, 9.

Harvati, K., 2003. The Neanderthal taxonomic position: models of intra- and interspecific craniofacial variation. Journal of Human Evolution 44, 107–132.

Harvati, K., Hublin, J.J., Gunz, P., 2010. Evolution of middle-late Pleistocene human cranio-facial form: a 3-D approach. Journal of Human Evolution 59, 445–464.

Hawks, J.D., Wolpoff, M.H., 2001. The accretion model of Neandertal evolution. Evolution International Journal of Organic Evolution 55, 1474–1485.

Hershkovitz, I., Smith, P., Sarig, R., Quam, R., Rodríguez, L., García, R., Arsuaga, J.L., Barkai, R., Gopher, A., 2011. Middle pleistocene dental remains from Qesem Cave (Israel). American Journal of Physical Anthropology 144, 575–592.

Hershkovitz, I., Weber, G.W., Fornai, C., Gopher, A., Barkai, R., Sloan, V., Quam, R., Yankel, G., Sarig, R., 2016. New Middle Pleistocene dental remains from Qesem Cave (Israel). Quaternary International 398, 148–158.
Hublin, J.J., 1998. Climatic changes, paleogeography, and the evolution of the Neanderthals. In: Akazawa, T., Aoki, K., Bar-Yosef, O. (Eds.), Neandertals and Modern Humans in Western Asia. Plenum, New York, pp. 295–310.
Kaifu, Y., Aziz, F., Baba, H., 2005. Hominid mandibular remains from Sangiran: 1952-1986 collection. American Journal of Physical Anthropology 128, 497–519.
Karkanas, P., Shahack-Gross, R., Ayalon, A., Bar-Matthews, M., Barkai, R., Frumkin, A., Gopher, A., Stiner, M.C., 2007. Evidence for habitual use of fire at the end of the Lower Paleolithic: site formation processes at Qesem Cave, Israel. Journal of Human Evolution 53, 197–212.
Keene, H.J., 1966. A morphologic and biometric study of taurodontism in a contemporary population. American Journal of Physical Anthropology 25, 208–209.
Krenn, V., 2015. Variation of 3D Outer and Inner Crown Morphology of Lower Premolars in Modern Humans (Masterthesis at the University of Vienna, Vienna).
Lieberman, D.E., McBratney, B.M., Krovitz, G., 2002. The evolution and development of cranial form in Homo sapiens. Proceedings of the National Academy of Sciences of the United States of America 99, 1134–1139.
Lucas, P.W., 2004. Dental Functional Morphology - How Teeth Work. Cambridge University Press, Cambridge.
Marcus, L.F., Corti, M., Loy, A., Naylor, G., Slice, D.E., 1996. Advances in Morphometrics [White Book]. Plenum Press, New York.
Martínez de Pinillos, M., Martinón-Torres, M., Skinner, M.M., Arsuaga, J.L., Gracia-Téllez, A., Martínez, I., Martín-Francés, L., Bermúdez de Castro, J.M., 2014. Trigonid crests expression in Atapuerca-Sima de los Huesos lower molars: internal and external morphological expression and evolutionary inferences. Comptes Rendus - Palevol 13, 205–221.
Martinón-Torres, M., Bastir, M., Bermudez de Castro, J.M., Gomez, A., Sarmiento, S., Muela, A., Arsuaga, J.L., 2006. Hominin lower second premolar morphology: evolutionary inferences through geometric morphometric analysis. Journal of Human Evolution 50, 523–533.
Martinón-Torres, M., Bermúdez De Castro, J.M., Gómez-Robles, A., Bastir, M., Sarmiento, S., Muela, A., Arsuaga, J.L., 2007. Gran Dolina-TD6 and Sima de los Huesos dental samples: preliminary approach to some dental characters of interest for phylogenetic studies. In: Bailey, S.E., Hublin, J.J. (Eds.), Dental Perspectives on Human Evolution. Springer, Berlin, pp. 65–79.
Martinón-Torres, M., Dennell, R., Bermudez de Castro, J.M., 2011. The Denisova hominin need not be an out of Africa story. Journal of Human Evolution 60, 251–255.
Martinón-Torres, M., Bermudez De Castro, J.M., Gómez-Robles, A., Prado-Simon, L., Arsuaga, J.L., 2012. Morphological description and comparison of the dental remains from Atapuerca-Sima de los Huesos site (Spain). Journal of Human Evolution 62 (1), 7–58.
Martinón-Torres, M., Spěváčková, P., Gracia-Téllez, A., Martínez, I., Bruner, E., Arsuaga, J.L., Bermúdez de Castro, J.M., 2013. Morphometric analysis of molars in a Middle Pleistocene population shows a mosaic of 'modern' and Neanderthal features. Journal of Anatomy 223 (4), 353–363.
Mercier, N., Valladas, H., Bar-Yosef, O., Vandermeersch, B., Stringer, C., Joron, J.L., 1993. Thermoluminescence date for the Mousterian Burial Site of Es-Skhul, Mt. Carmel. Journal of Archaeological Science 20, 169–174.
Mercier, N., Valladas, H., Falgueres, C., Shao, Q., Gopher, A., Barkai, R., Bahain, J.J., Vialettes, L., Joron, J.L., Reyss, J.L., 2013. New datings of Amudian layers at Qesem Cave (Israel): results of TL applied to burnt flints and ESR/U-series to teeth. Journal of Archaeological Science 40 (7), 3011–3020.
Meyer, M., Kircher, M., Gansauge, M.T., Li, H., Racimo, F., Mallick, S., Schraiber, J.G., Jay, F., Prüfer, K., De Filippo, C., Sudmant, P.H., Alkan, C., Fu, Q., Do, R., Rohland, N., Tandon, A., Siebauer, M., Green, R.E., Bryc, K., Briggs, A.W., Stenzel, U., Dabney, J., Shendure, J., Kitzman, J., Hammer, M.F., Shunkov, M.V., Derevianko, A.P., Patterson, N., Andrés, A.M., Eichler, E.E., Slatkin, M., Reich, D., Kelso, J., Pääbo, S., 2012. A high-coverage genome sequence from an archaic Denisovan individual. Science 338, 222–226.
Mitteroecker, P., Gunz, P., Bernhard, M., Schaefer, K., Bookstein, F.L., 2004. Comparison of cranial ontogenetic trajectories among great apes and humans. Journal of Human Evolution 46, 679–697.
Molnar, S., 1971. Human tooth wear, tooth function and cultural variability. American Journal of Physical Anthropology 34, 175–189.
Noonan, J.P., Coop, G., Kudaravalli, S., Smith, D., Krause, J., Alessi, J., Chen, F., Platt, D., Pääbo, S., Pritchard, J.K., Rubin, E.M., 2006. Sequencing and analysis of Neanderthal genomic DNA. Science 314, 1113–1118.
Parfitt, S.A., Ashton, N.M., Lewis, S.G., Abel, R.L., Coope, G.R., Field, M.H., Gale, R., Hoare, P.G., Larkin, N.R., Lewis, M.D., Karloukovski, V., Maher, B.A., Peglar, S.M., Preece, R.C., Whittaker, J.E., Stringer, C.B., 2010. Early pleistocene human occupation at the edge of the boreal zone in northwest Europe. Nature 466, 229–233.
Parush, Y., Assaf, E., Slon, V., Gopher, A., Barkai, R., 2015. Looking for sharp edges: modes of Flint recycling at Qesem Cave, Israel: report on work-in-progress. Quaternary International 361, 61–87.
Ponce de Leon, M.S., Zollikofer, C.P., 2001. Neanderthal cranial ontogeny and its implications for late hominid diversity. Nature 412, 534–538.
Prüfer, K., Racimo, F., Patterson, N., Jay, F., Sankararaman, S., Sawyer, S., Heinze, A., Renaud, G., Sudmant, P.H., De Filippo, C., Li, H., Mallick, S., Dannemann, M., Fu, Q., Kircher, M., Kuhlwilm, M., Lachmann, M., Meyer, M., Ongyerth, M., Siebauer, M., Theunert, C., Tandon, A., Moorjani, P., Pickrell, J., Mullikin, J.C., Vohr, S.H., Green, R.E., Hellmann, I., Johnson, P.L.F., Blanche, H., Cann, H., Kitzman, J.O., Shendure, J., Eichler, E.E., Lein, E.S., Bakken, T.E., Golovanova, L.V., Doronichev, V.B., Shunkov, M.V., Derevianko, A.P., Viola, B., Slatkin, M., Reich, D., Kelso, J., Pääbo, S., 2014. The complete genome sequence of a Neanderthal from the Altai Mountains. Nature 505, 43–49.
Quam, R., Bailey, S., Wood, B., 2009. Evolution of M1 crown size and cusp proportions in the genus Homo. Journal of Anatomy 214, 655–670.
Reich, D., Green, R.E., Kircher, M., Krause, J., Patterson, N., Durand, E.Y., Viola, B., Briggs, A.W., Stenzel, U., Johnson, P.L.F., Maricic, T., Good, J.M., Marques-Bonet, T., Alkan, C., Fu, Q., Mallick, S., Li, H., Meyer, M., Eichler, E.E., Stoneking, M., Richards, M., Talamo, S., Shunkov, M.V., Derevianko, A.P., Hublin, J.J., Kelso, J., Slatkin, M., Pääbo, S., 2010. Genetic history of an archaic hominin group from Denisova cave in Siberia. Nature 468, 1053–1060.
Rightmire, G.P., 2008. Homo in the middle pleistocene: hypodigms, variation, and species recognition. Evolutionary Anthropology 17 (1), 8–21.
Roebroeks, W., Villa, P., 2011. On the earliest evidence for habitual use of fire in Europe. Proceedings of the National Academy of Sciences of the United States of America 108 (13), 5209–5214.
Santa Luca, A.P., 1978. A re-examination of presumed Neanderthal-like fossils. Journal of Human Evolution 7, 619–636.
Schwarcz, H.P., Buhay, W.M., Grün, R., Valladas, H., Tchernov, E., Bar-Yosef, O., Vandermeersch, B., 1989. ESR dating of the Neanderthal site, Kebara Cave, Israel. Journal of Archaeological Science 16, 653–659.
Schwartz, J.H., Tattersall, I., 1996. Significance of some previously unrecognized apomorphies in the nasal region of Homo neanderthalensis. Proceedings of the National Academy of Sciences of the United States of America 93, 10852–10854.
Shahack-Gross, R., Berna, F., Karkanas, P., Lemorini, C., Gopher, A., Barkai, R., 2014. Evidence for the repeated use of a central hearth at Middle Pleistocene (300ky ago) Qesem Cave, Israel. Journal of Archaeological Science 44 (1), 12–21.
Shimelmitz, R., Barkai, R., Gopher, A., 2011. Systematic blade production at late Lower Paleolithic (400-200 kyr) Qesem Cave, Israel. Journal of Human Evolution 61, 458–479.
Shimelmitz, R., Barkai, R., Gopher, A., 2016. Regional variability in Late Lower Paleolithic Amudian Blade Technology: analyzing new data from Qesem, Tabun and Yabrud I. Quaternary International 398, 37–60.
Smith, F., 1984. Fossil hominids from the Upper Pleistocene of central Europe and the Origin of Modern Europeans. In: Smith, F., Spencer, F. (Eds.), The Origins of Modern Humans. Alan R. Liss, New York, pp. 137–209.
Stiner, M., Gopher, A., Barkai, R., 2009. Cooperative hunting and meat sharing 400-200 kya at Qesem Cave, Israel. Proceedings of the National Academy of Sciences U.S.A 106, 13207–13212.
Stiner, M., Gopher, A., Barkai, R., 2011. Hearth-side socioeconomics, hunting and Paleoecology during the Late Lower Paleolithic at Qesem Cave, Israel. Journal of Human Evolution 60, 213–233.
Stringer, C., 2012. The status of Homo heidelbergensis (Schoetensack 1908). Evolutionary Anthropology 21, 101–107.
Stringer, C.B., Andrews, P., 1988. Genetic and fossil evidence for the origin of modern humans. Science 239, 1263–1268.
Suzuki, H., Takai, F., 1970. The Amud Man and His Cave Site. University of Tokyo Press, Tokyo.
Trinkaus, E., 1984. Western Asia. In: Smith, F., Spencer, F. (Eds.), The Origins of Modern Humans. Alan R. Liss, New York, pp. 251–325.
Turner, C.G., N, C.R., Scott, G.R., 1991. Scoring procedures for key morphological traits of the permanent dentition: the Arizona State University Dental Anthropology System. In: Kelley, M., Larsen, C. (Eds.), Advances in Dental Anthropology. Wiley-Liss, New York, pp. 13–31.
Valladas, H., Mercier, N., Froget, L., Hovers, E., Joron, J.L., Kimbel, W.H., Rak, Y., 1999. TL dates for the Neanderthal site of the Amud Cave, Israel. Journal of Archaeological Science 26, 259–268.
van Asperen, E.N., 2012. Late Middle Pleistocene horse fossils from northwestern Europe as biostratigraphic indicators. Journal of Archaeological Science 39, 1974–1983.
Vlcek, E., 1993. Fossile Menschenfunde von Weimar-Ehringsdorf (Kommissionsverlag Konrad Theiss Verlag, Stuttgart).
Vlcek, E., 2011. Die Zähne des fossilen Menschen von Bilzingsleben. Praehistoria Thuringica. Beier und Beran, Langenweißbach, pp. 80–122, 13.
Vlcek, E., Mania, D., Mania, U., 2002. Der fossile Mensch von Bilzingsleben. Beier & Beran, Weissbach.
Wagner, G.A., Krbetschek, M., Degering, D., Bahain, J.J., Shao, Q., Falguères, C., Voinchet, P., Dolo, J.M., Garcia, T., Rightmire, G.P., 2010. Radiometric dating of the type-site for Homo heidelbergensis at Mauer, Germany. Proceedings of the National Academy of Sciences of the United States of America 107, 19726–19730.
Weber, G.W., 2015. Virtual Anthropology. Yearbook of Physical Anthropology. http://dx.doi.org/10.1002/ajpa.22658.
Weber, G.W., Bookstein, F.L., 2011. Virtual Anthropology - a Guide to a New Interdisciplinary Field. Springer Verlag, Wien, New York, ISBN 978-3-211-48647-4.
Wrangham, R., 2009. Catching Fire: How Cooking Made Us Human. Basic Books, New York.
Zanolli, C., Mazurier, A., 2013. Endostructural characterization of the H.heidelbergensis dental remains from the early middle pleistocene site of Tighenif, Algeria. Comptes Rendus - Palevol 12, 293–304.